Vol. 9, №1, 2025 ISSN 2520-6133

KHAZAR JOURNAL OF SCIENCE AND TECHNOLOGY

(KJSAT)

Hamlet Isayev/Isaxanli[1] *

Editor-in-Chief Khazar University, Azerbaijan

[1] Also H. Issakhanly, H. Isakhanly, H. Isakhanli, H.A.Isayev, G.A.Isayev, or G.A.Isaev due to differences in transliteration. I use Hamlet Isayev in mathematics and science fields and Hamlet Isakhanli/Isaxanli in humanities.

Khazar University
41 Mehseti str., Baku AZ1096 Republic of Azerbaijan Tel: (99412) 4217927
Website: **www.kjsat.com**

KHAZAR UNIVERSITY PRESS

Content

Khazar Journal of Science and Technology `Volume 9 №1 2025, 5-14
 DOI: 10.5782/2520-6133.2025.9.1.5

Analysis of Physico-Chemical Parameters of Drinking Water from Kur River, Azerbaijan

[1]Fidan Yolchuyeva, [1]Sevinj Hajiyeva, [2]Ali Huseynli
[1]Ecological Chemistry Department, Baku State University
[2]Mathematics Department, Khazar University
Corresponding author: ahuseyinli@yahoo.com

Abstract
The present study was conducted to determine the physicochemical parameters of drinking water. The samples were collected from six sites along the Kur River. We have analyzed some physicochemical parameters such as pH, Electrical conductivity (EC), Total dissolved solids (TDS), Total alkalinity (TA), Chloride (Cl^-), fluoride (F^-) and others. Results showed that the physicochemical parameters of drinking water were also within the normal range.

Keywords: physicochemical parameters, drinking water, Kur river

Introduction

Drinking water is distributed unevenly in Azerbaijan, with limited resources. At present, the country's surface water reserves are 27 cubic meters, while in dry years these reserves are reduced to 20-21 cubic kilometers. The sources of surface water resources are rivers, lakes, reservoirs and glaciers. 70-72% of the freshwater resources of our country are formed outside the country (Badalov, 2016).

In the 1960s, the demand for drinking water in the Absheron peninsula increased sharply as a result of the construction of new residential areas and micro-districts in Baku and the growth of surrounding villages and villages. The Binagadi district we take as a research site is located in the northwest of the Absheron Peninsula. Its territory is 169.38 km2 and the population is 1496 people per 1 km2. According to 2014 statistics, the population of Binagadi district is 254,500.

Binagadi district is currently supplied with drinking water from three sources - Oguz-Gabala, Kura and Jeyranbatan (Aliyev, 2000).

Kura is a source of drinking water for 60-70% of the republic's population. It is a vital factor for the population, agriculture and industry of our republic. From this point of view, the analysis of the contamination of the Kur River in Azerbaijan is of great importance (Tagiev et al., 2001).

Samples were taken from the Kur River to test the quality of drinking water supplied to the Binagadi area. The Kur River, the largest transboundary river in the Caucasus, is located in five countries, and its water is used for various purposes. As a result, the Kur River is exposed to both natural and anthropogenic effects. There are about 30 transboundary rivers in the Kur basin. The largest of these is the Araz River (Aslanov, 2013). The total water reserve of the Kur River is 25.9 km.3, of which 9.39 km^3 belongs to Georgia, 4.6 km^3 to Azerbaijan and 1.54 km^3 to Armenia. The main water users in the downstream zone of the Kura River are irrigation and water supply. Thus, 7335 million m3 of water (7214 million m^3 of water and 122 million m^3 of drinking water) is extracted from the Kura River in the republic, of which 3160 million m^3 falls on the downstream zone (Aslanov and Huseynova-Javadova, 2005). During periods of high water demand, water from the rivers, which is irreversible, contributes to the deterioration of the ecosystem. Reservoirs built on the basin also have a significant impact on water flow (Aslanov et al., 2012).

The Kura River is exposed to severe pollution primarily due to industrial and municipal waste from other settlements in Georgia. As a result, the Kura river enters our republic as a highly contaminated river, which is dangerous for human and aquatic organisms (Aslanov et al., 2005). The Khramchai Kura, the right arm of the Kura, which runs along the border of the two republics, brings a lot of wastewater. In Georgia, the Khram River is joined by the most polluted river of Armenia - the Debed River. Industrial and domestic wastes from these cities are discharged into the river without treatment (Huseynov and Imanov, 2017; Ismayilov and Karimov, 2012).

Methodology

Drinking water samples were collected from Kur river for the analysis of their physicochemical parameters. Six samples of water were collected from the Kur river in a plastic bottle. Samples taken to the laboratory have been analyzed some physico-chemical parameters such as pH, Electrical conductivity (EC), Total dissolved solids (TDS), Total alkalinity (TA), Chloride (Cl^-), fluoride (F^-) and others. (Table 1.)

Table 1. Analysis method of samples

Water quality test	Description	Instrument/ method
pH	Determination of hydrogen ions in water	pH meter
Electrical conductivity	Numerical expression of the electrical conductivity of a solution	Conductivity meter
Total Hardness	Determination of calcium and magnesium in water	Titrimetric method
Total Alkalinity	Alkalinity of water is its quantitative capacity to react with a strong acid to a designated pH.	Titrimetric method
Chloride	Measurement of Chloride amount in water	Titrimetric method
Sulfate	Measurement of Sulfate amount in water	Titrimetric method
Nitrate	Measurement of Nitrate amount in water	Titrimetric method

Results and discussion

pH

The pH is a measure of the hydrogen ion concentration in water. First of all, the device is calibrated. After calibration, the pH of the water samples was measured. The heat affects the pH. As the temperature increases, the characteristics of the electrode change. The curve increases with increasing heat and an error occurs on the device. Therefore, sample analysis and calibration solutions should be performed at room temperature. When electrodes are not used, they should be stored in KCl solution of 0.1M. The pH in drinking water should be in the range of 6.5-8.5. uric acid causes corrosion. Alkaline water becomes bitter. It ranges from 8.07-8.30 in the samples taken in this analysis. It complies with WHO and 98/83 EC directive standards (WHO, 2004): Guidelines for drinking water quality. 3rd edn. World Health Organization, Geneva.). This amount does not adversely affect human health. (Figure1)

.

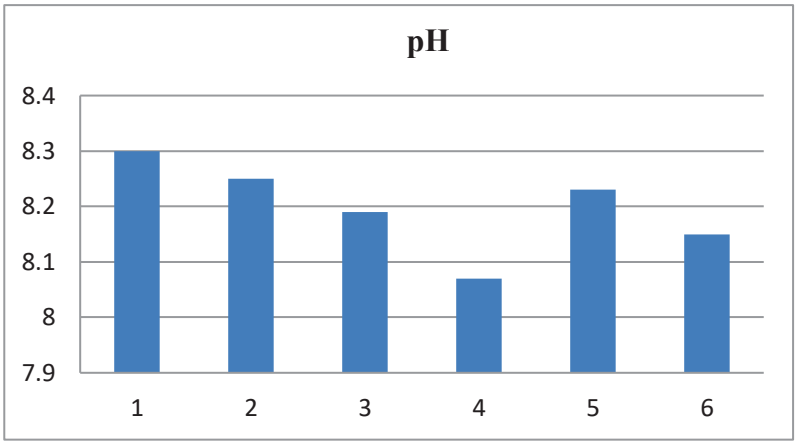

Figure1. pH of drinking water samples from Kur river Azerbaijan

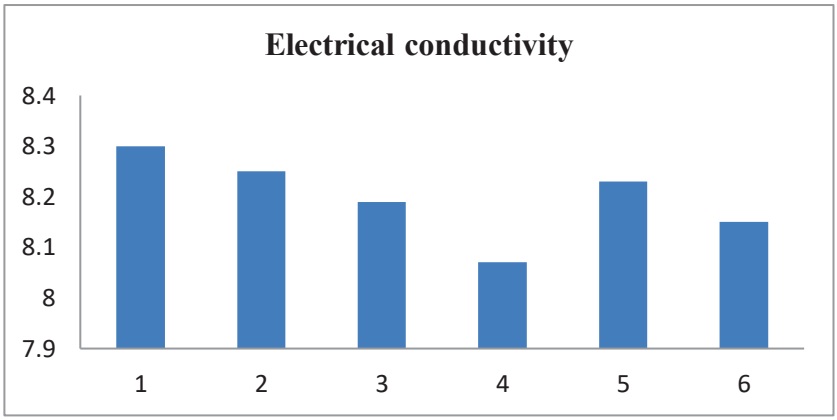

Figure 2. Electrical conductivity of drinking water samples from Kur river Azerbaijan

Turbidity

It is based on measuring the intensity of light emitted by the particles of a substance by nephrometric method. Turbidity should be measured quickly. If this is not possible, the sample should be kept at 4 ° C for 24 hours in the dark. Thermal fluctuations and particle collapse may be an error in the analysis.

Electrical Conductivity (EC)

Conductivity was measured using conductivity meter. Conductivity meter was calibrated using 0.1 molar of KCl. Electric conductivity is a numerical

expression of the ability of aqueous solution to conduct electricity. In our samples, the electrical conductivity is 723-1155 μS / cm.Conductivity of drinking water samples is given Table 2 and shown Figure 2. The conductivity of water is affected by the suspended impurities and also depends upon the concentration of ions in the water. (Figure 2).

Total Alkalinity (TA)

It is derived from hydroxide, carbonate and bicarbonate ions. Sodium thiosulaft solution is added. An indicator of phenolphthalein is being added. When the solution turns pink, the solution is vibrated with 0.02 N HCl until it is discolored. With 0.02 N HCl, a pointer may be added to analyze the overall look so you can see the color without the blue-green color. The alkaline content in the samples is 2.6-3.58 mg / L (Figure 3).

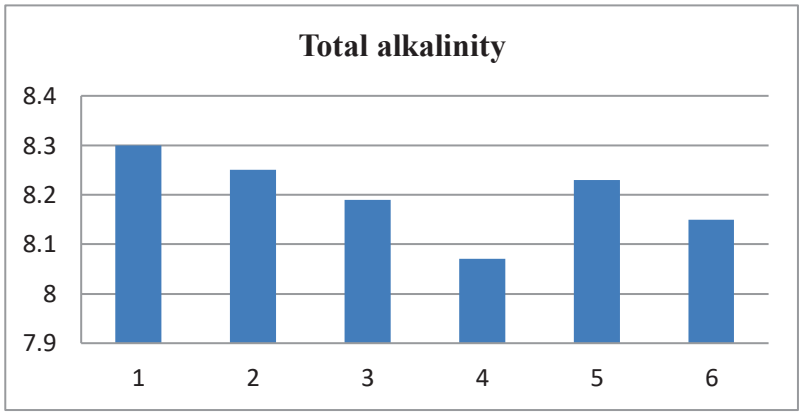

Figure 3. Total Alkalinity of drinking water samples from Kur river Azerbaijan.

Total Dissolved Solids (TDS)

The sample is passed through a glass fiber filter and heated until the filtrate dries. The increase in the weight of the container indicates the presence of solids in the sample. When the sample contains too much calcium, magnesium chloride or sulphates, it increases the hygroscopicity of the sample. This reduces the accuracy of the analysis. For this you need to dry the sample even more. According to WHO standards, the tolerance for TDS should not exceed 500 mg / L. In the samples, the TDS ranges from 486-724 mg / L (Figure 4).

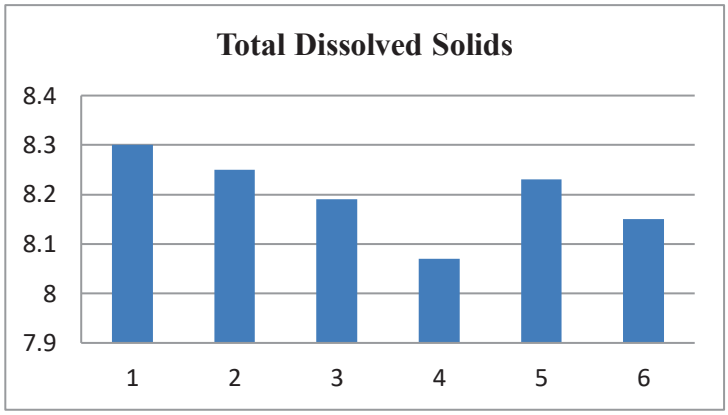

Figure 4. Total Dissolved Solids of drinking water samples from Kur river Azerbaijan

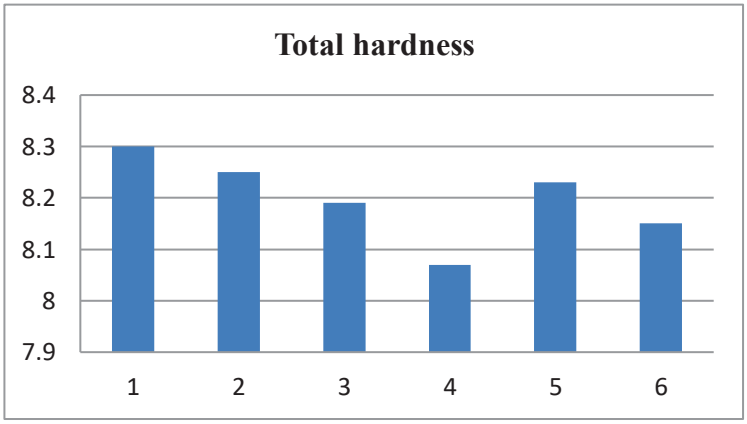

Figure 5. Total Hardness of drinking water samples from Kur river Azerbaijan.

Total hardness (TH)

Total hardness is mainly contributed by bircarbonates, carbonates, sulphates and chlorides of calsium and magnesium. 50 ml of the sample is added 1-2 ml of buffer solution (ammonium chloride, ammonium hydroxide mixture) and 2-3 drops of eryochrome black T indicator. The solution is colored red. The mixture is then vibrated with the EDTA solution until light blue. Finally the total hardness of the water samples was determined in mg / L og CaCO3. In the samples we take, TH varies between 239-348 mg / L. According to Who standards, TH must not exceed TH 500 mg / L in drinking water. According to magic, water is subdivided into soda and multiple cod waters (Figure 5).

Chloride

50 ml of sample is taken for testing. For example, the pH value should change in the range of 7-10. if the pH is not within this range, it is reached with 1N NaOH or 1 H_2SO_4 solution. The mixture is then titrated with the indicator K_2CrO_4. Vibrating is done until pink is obtained. Finally, the amount of chloride in the sample is calculated by the following formula.

$$\text{Concentration of chloride (mg/l)} = \frac{(A - B) \cdot N \cdot f \cdot 35450}{\text{V samples}}$$

A- The amount of silver nitrogen used for the sample,
B- The amount of silver nitrate used for the blank,
N- normality of silver nitrate solution,
V- sample volume

The concentration of chlorine ions in the samples varied in the range of 37.5-92 mg / L. According to 98/38 EC and WHO standards, the amount of chlorine ions in drinking water should not exceed 250 mg / L (Figure 6).

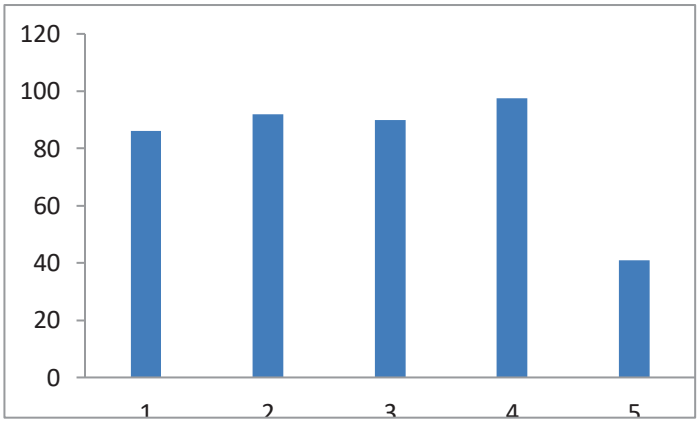

Figure 6. Chloride of drinking water samples from Kur river Azerbaijan.

Sulfate analysis

It is based on measuring the adsorption value of $BaSO_4$ suspension at wavelengths of 420 nm on a spectrophotometer. The buffer solution containing $MgCl_2 \cdot 6H_2O$, $CH_3COONa \cdot 3H_2O$, KNO_3, CH_3COOH was used in the process. 20 ml buffer solution is added to 100 mL of sample. The mixture is placed in the Kuwait and resuspended on a wavelength

spectrophotometer at 420 nm. Then pour the recyclable tube and weigh it by adding about 0.2 g of $BaCl_2 \cdot 2H_2O$. According to the standards 98/38 / EC, the amount of sulfate ions in drinking water should not exceed 250 mg / L. In our samples, the lowest concentration of sulfate ions was 165 mg / L. In some examples, this figure is 275 mg / L. This is higher than the standards (Figure 7).

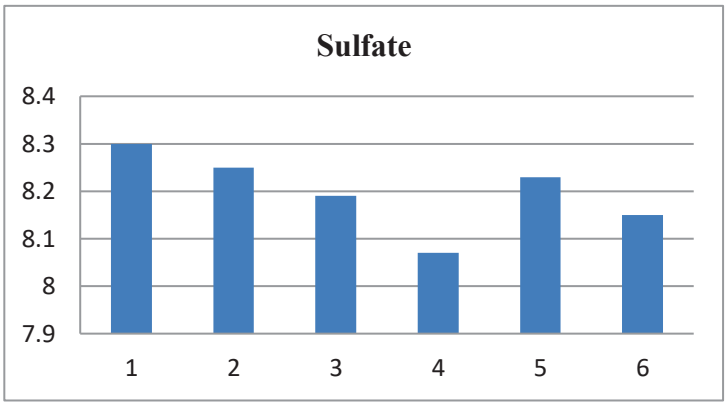

Figure 7. Sulfate of drinking water amples from Kur river Azerbaijan

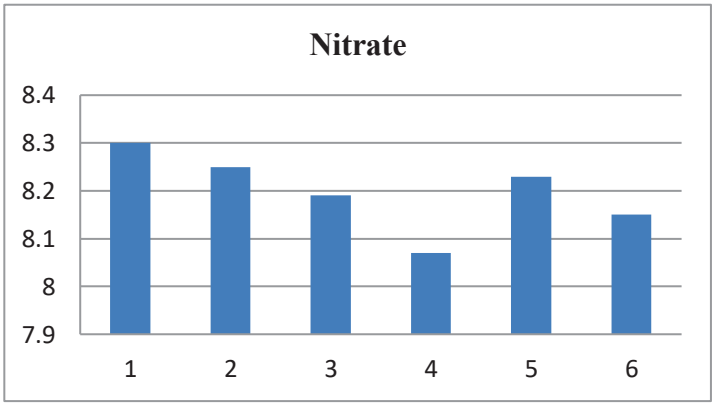

Figure 8. Nitrate of drinking water samples from Kur river Azerbaijan.

Nitrate analysis

The spectrophotometer is analyzed at wavelengths of 220-275 nm. In the process, stock nitrate solution containing 100 mg / L nitrogen and 1 N hydrogen chloride solution were used. (1 ml of 1N HCl solution is added to 50 ml sample). The amount of nitrate ions in the samples ranges from 3.1-4.5 mg / L. According to the standards 98/38 / EC, the amount of nitrate ions in drinking water should not exceed 45 mg / L.

Conclusion

This article deals with the analysis of the physiochemical parameters of water samples taken from the Kura River, which plays a major role in providing potable water to the population in Azerbaijan. The pH, electrical conductivity, TDS, TA, TH, sulfates, chlorides, nitrates, fluorides and some other parameters were determined in the samples. The results were compared with the requirements of the World Health Organization and Directive 98/38 / EC on potable water.

Table 2. All analysis results are listed

	Sample1	Sample2	Sample3	Sample4	Sample5	Sample6	WHO	98/38/EC
pH (pH unit)	8.30	8.25	8.19	8.07	8.23	8.15	6,5-8,5	
Turbitidy (NTU)	53.6	0.90	1.1	8.34	11.2	5.4	-	1
Conductivity (µS/sm)	1116	1151	1155	723	751	724	-	< 2500 (20^0C)
Total Hardness (mg/L)	331	344	348	242	247	239	500 mg/L-	-
Total Dissolved Solids(mg/L)	724	726	730	472	464	486	500 mg/L	-
T.Alkalinity (mg/L)	3.58	3.35	3.28	2.6	2.9	3.1		
Chloride (mg/L)	86	92	90	97.5	41	38	-	250 mg/L
Nitrate (mg/L)	3.9	4.1	4.5	3.8	3.5	3.1	-	45 mg/L
Sulfate (mg/L)	265	275	273	167	173	165	-	250 mg/L
Fluoride (mg/L)	0.2	0.3	0.2	0.14	0.19	0.22	-	1,5

Based on the analysis results, the water samples taken are suitable for drinking. pH 8.07-8.30 in the samples; TA 2.6-3.58 mg / L; TDS was 486-724 mg / L, TH 239-348 mg / L, sulfates 165 -275 mg / L, chlorides 37.5-92 mg / L, nitrates 3.1-4.5 mg / L. Although sulfate levels are slightly high, they are not harmful to health. Although it breaks down the intestines in non-habitual people, the digestive system is accustomed to it over time.

This work was carried out with the financial support of the Azerbaijan Science Foundation-Grant №AEF-MQM-QA-1-2021-4(41)-8/07/4-M-07.

References

Aliyev, F.Sh. (2000). Groundwater, resources use and geological problems of the Republic of Azerbaijan. Baku, Chashoglu.

Aslanov, H.Q. (2013). Ecogeographical problems of downstream Kura, "Chashioglu", Baku.

Aslanov, H.Q & Huseynova-Javadova Sh.N. (2005). Ecology and Water Management. №7, Baku.

Aslanov, H.K & Samkhalova, A.P. (2005). Natural conditions and ecological features of the Kura river basin. Ecology and Water Resources, №3.

Aslanov, H.Q & Javadova Sh.H. (2005). Natural and Anthropogenic Factors Affecting the Concentration of the Kura River Sources. Proceedings of the XXVI Scientific Conference of Students and Masters of ASU.

Badalov, E. (2016). Socio-demographic problems and settlement issues in Absheron economic-geographical region. European publishing house.

Fatullayev, G.Yu. (2002). Recurrent changes of water resources and regime in the South Caucasus (in the Caspian Basin). Baku.

Huseynov, G.J & Imanov, F.A. (2017). The role of Kura river in water supply and antropogenic changes of annual flow..“Water resources, hydraulic facilities and environment” materials of the international scientific-practical conference.

Ismayilov, R.A & Karimov, R.N. (2012). Evaluation of Contemporary Environmental Condition of River Basins in Southern pre-Caspian Areas of Azerbaijan. International Journal of Business, Humanities and Technology.USA- Vol. 1 № 1.

Tagiev, I.I., Ibragimova, I.Sh. & Babaev, A.M. (2001). Mineral resources and terminal valleys of Azerbaijan. Baku, Chashoglu.

WHO. (2004). Guidelines for drinking water quality. 3rd edn. World Health Organisation, Geneva.

Khazar Journal of Science and Technology `Volume 9 №1 2025, 15-20
 DOI: 10.5782/2520-6133.2025.9.1.15

Ecological Analysis of the Causes of the Formation of Ecotoxicant H_2S and SO_2 Compounds in the Secondary Steel Melting Industry

Naila Jafarova, Sevinj Hajiyeva, Giyas Bayramov
Ecological Chemistry Department, Baku State University, Baku,Azerbaijan
Corresponding author: ceferova-nailem@mail.ru

Abstract
In many literature sources, the reasons for the formation and emission of harmful substances in the Primary and Secondary Steel Melting production areas are often not analyzed in detail. Based on the information provided in some literature, we conducted ecological research and explanations regarding the reasons for the formation of H_2S and SO_2 gases, considered ecotoxicants, in the atmospheric air and wastewater at the Secondary Steel Melting Plant. The causes of the formation of H_2S and SO_2 compounds in Secondary Steel Melting production were studied, and their ecological scientific explanations were justified. As is known, after some time, every waste leads to pollution in the lithosphere, hydrosphere, and atmosphere, which ultimately has negative impacts on the biosphere, especially on human health. In this regard, our scientific research focused on providing ecological scientific explanations for the reasons for the formation of each harmful substance at the Secondary Steel Melting Plant, which is one of the most important issues.
Keywords: ecotoxicant, steel melting, ecological analysis, Electric Arc Furnace, working zone, maximum allowable concentration

Introduction

As is known from many technical literature sources (Mammadov, 2012; Eyvazov, 2014), the Secondary Steel Melting Plant is significant both ecologically and economically. In the metallurgical industry, steel melting initially results in the release of more harmful substances into the atmosphere, leading to higher consumption of energy resources and natural ore reserves. However, it should be noted that less natural ore is used in relation to Secondary Steel Melting (Shukurov, 2002). Despite this, at the Secondary Steel Melting Plant, many waste materials, especially with wastewater, are released into the atmosphere as harmful substances. The amount of harmful substances emitted into the atmosphere is significantly lower compared to primary steel melting.

According to modern ecological requirements (Guliyev et al., 2003), environmental protection is one of the most important ecological demands of the day. One of the main causes of environmental pollution is the melting of old, unusable metal waste. As mentioned earlier, despite the advantages of the Secondary Steel Melting sector over the Primary Steel Melting sector, this industry is also considered one of the major sources that pollute the environment in various directions. In many cases (Eyvazov, 2014), the melting of alloys in the Secondary Steel Melting sector leads to poor-quality metal alloys. One of these factors is the presence of mercury compounds in the alloys, which have toxic effects on the human body and can even result in death. Another factor is the presence of tungsten-containing metal waste, which requires very high temperatures and additional costs during melting. Therefore, these types of metal waste are considered unusable waste.

It can be noted that when using reagents containing sodium compounds, the reaction with water leads to the formation of hydrogen and combustible flames, which negatively affects the quality of the metal alloy. Additionally, according to the information provided by the enterprise, research has shown that excessive use of certain reagents results in the production of low-quality alloys. Despite these factors, it should be emphasized that the materials obtained at the Secondary Steel Melting Plant play a crucial role in the construction industry, particularly in the production of special reinforcement and equipment. The concentrations of H_2S and SO_2 compounds present in both the wastewater generated in the Baku Steel Melting Plant's Electric Arc Furnace (EAF) and related production areas, as well as those released into the atmosphere, were measured using a Drager Tubes LLG gas detector, a highly sensitive mobile device.

Materials and methods

During the ecological research conducted at the Baku Steel Melting Plant, the actual concentrations of H_2S and SO_2 gases in the air were determined within the area of the Electric Arc Steel Melting Furnace (EAF) and its surroundings, along with other ecotoxicant substances.

Table 1. Analysis Results of Ecotoxicant Inorganic Substances Emitted into the Atmosphere from the EAF

Name of ecotoxicant characteristic inorganic substances	Their maximum allowable concentration (MAC) mg/m3	Concentrations determined in the EAF
H_2S	0.008	10 ppm (13.93 mq/m^3)
SO_2	0.05	5 ppm (13.01 mq/m^3)

The determination of the concentrations of ecotoxicant substances in the air was carried out using glass indicator tubes.The analyses were repeated several times on different days to refine the average values. Measurements were conducted at distances of 10–50 meters from the Electric Arc Steel Melting Furnace (EAF) area of the plant. Due to the plant's ventilation system, the results of these analyses showed some variations. Therefore, based on the average values, the results of the analysis of these harmful substances are presented in Table 1.

As seen in Table 1, the one-time maximum concentration of H_2S was high. According to literature data, the one-time Maximum Allowable Concentration (MAC) of H_2S and SO_2 gases in the air should be ≤ 10 mg/m³. However, in the initial state, the concentration of these harmful substances in the studied areas was significantly higher. Due to the rapid operation of the plant's ventilation system, the concentration of these substances decreases over short periods and reaches the Long-Term Allowable Concentration (LAC) at greater distances from the sources.In the working zone of the EAF area at the studied plant, the concentrations of ecotoxicant inorganic pollutants in the air were determined at distances of 50, 100, 150, and 200 meters, as well as in sanitary protection zones. The obtained results are presented in Table 2.

Table 2. Analysis Results of Ecotoxicant Inorganic Substances in the Atmospheric Air Outside the EAF

Name of ecotoxicant characteristic inorganic substances	Concentrations determined outside the EAF				
	50 m	100 m	150 m	200 m	Sanita mühafizə zonasında
H_2S	8 ppm	7 ppm	5 ppm	2.5 ppm	2 ppm
SO_2	4.1 ppm	2.2 ppm	1.7 ppm	1.0 ppm	1.5 ppm

The ecotoxicant substances emitted into the atmosphere from the Baku Steel Melting Industry Plant can spread not only up to 1 km but, depending on meteorological conditions, can actually disperse over distances of hundreds of kilometers.

In technical literature, particularly in the Secondary Steel Melting Industry, there are no scientific explanations provided for the causes of the formation of H_2S and SO_2 ecotoxicant compounds. Based on the results of long-term

research conducted in the production areas and the information about the reagents used in those areas, the following scientific explanations can be provided:

1. In the Secondary Steel Melting Industry, the presence of up to 2% sulfur in petroleum coke leads to the release of sulfur in its free form at high temperatures (≤ 1500°C) during the steel melting process. At the same time, the decomposition of hydrocarbons in petroleum coke results in the release of hydrogen. (G.I. Bayramov, A.A. Samadova, N.M. Jafarova, 2019)

$$H_2 + S \rightarrow H_2S$$

At high temperatures, H_2S reacts with air to form:

$$H_2S + \text{air} \rightarrow SO_2; \text{ likely } SO_3; S; NxOy$$

This process results in the formation of harmful substances.

2. In the Secondary Steel Melting Industry, when the metal waste containing sulfur, which is no longer suitable for use, is melted, a certain amount of sulfur is released. This leads to the formation of H_2S and sulfur gas according to the reaction mechanism mentioned above.

At the Baku Steel Melting Plant, the analysis of construction reinforcement bars obtained after secondary steel melting is carried out regularly by the plant. The X-ray spectra and X-ray diffraction spectra of the solid slag waste formed at the plant have been studied using the S8 Tiger and Miniflex 600 devices. The obtained results are presented in Table 3.

Table 3. Chemical Composition, in %

Sample's conditional name	MgO	SiO_2	SO_3	P_2O_5	CaO	TiO_2	MnO	Fe_2O_3	Cr_2O_3
I furnace alkaline	3.19	21.60	0.24	0.66	31.43	0.58	6.07	28.81	2.10
II furnace alkaline	1.86	20.19	0.32	0.65	41.50	0.68	5.50	21.15	2.03

As seen from the tables, despite the high-temperature melting of metal waste, the composition still contains the metal oxides mentioned above, as well as sulfur compounds. Therefore, it can be stated that the ecological explanation provided for the formation of ecotoxicant sulfur compounds in the Secondary Steel Melting Plant is scientifically justified.

Result

As known from the literature (Mukuldev, 2018), the primary objective of conducting any ecological scientific research in a plant is to determine the formation of waste with varying composition and quantity, depending on the raw material composition and the technological process used. It is important to note that, alongside the in-depth determination of the composition and environmental impact of each waste, the theoretical and practical explanation of the causes of waste generation is considered a key indicator of the research work.

The results of the conducted ecological scientific research and ecological study can be noted as follows:

1. The formation of H_2S and SO_2 gases in the Secondary Steel Melting Industry has been scientifically and theoretically justified.
2. The main reasons for the formation of H_2S and SO_2 compounds in the Secondary Steel Melting Industry are primarily due to the presence of sulfur in the petroleum coke used for steel melting. Additionally, the use of sulfur-iron compounds as raw materials in the Electric Arc Steel Melting Furnace (EAF) results in the formation of H_2S and SO_2 gases.
3. At the Baku Steel Melting Plant, due to the melting of various types of metal waste, including sulfur-containing non-ferrous and ferrous metals, a significant amount of H_2S and SO_2 compounds are formed.
4. It should also be noted that, during secondary steel melting in the EAF, the concentrations of ecotoxicant substances released into the air from the working zone are found to be many times higher than the Maximum Allowable Concentration (MAC) within an area of up to 10 km (Romanov and Romanova, 2020)

Therefore, considering the above, we propose that the final stage of the ventilation system should involve the neutralization or absorption of H_2S and SO_2 gases in a gas scrubber using special adsorbent solutions, such as NaOH or $Ca(OH)_2$. Based on this proposal, it would be possible to use large amounts of CaS and Na_2S salts in the production of sulfuric acid.

References

Aliyeva, R.A., & Hajiyeva, S.R. (2009). Weighing and analysis of samples. Baku, p.116.

Bayramov, G.I., Samadova, A.A., & Jafarova, N.M. (2019). "Methods of Analysis of Harmful Substances in the Industrial Waste Water Produced in the Oil Industry", Methodological Manual, Baku, p. 26.

Eyvazov, B.Y. (2014). Ecology of Metallurgical Processes, Baku, Education, 260 pages.

Guliyev, A.H. (2003). Steel Castings, Baku, AzTU, 360 pages.

Mammadov, R. (2012). Azerbaijan's Metallurgical Industry and Its Development Perspectives. Xalq Newspaper, 3-4.

Mirbabayev, M. (2015). Ecology of Airspace, Baku, AzTU, 140 pages. (in Azeri)

Mukuldev, K. (2018). Process Waste Generation and Utilization in Steel Industry, International Journal of Industrial and Manufacturing Systems Engineering. 3(1), 1-5.

Orekhova, A.N. (2015). Environmental Issues of Foundry Production. Production Ecology. No.4, p.23-27.

Romanov, V., & Romanova, R. (2020). Emissions of Harmful Substances and Their Dangers to Living Organisms, LitRes.

Shukurov, R.I. (2002). Metallurgy, Baku, 450 pages. (in Azeri)

Shukurov, R.I., & Rahimov, M.M. (2005). Metallurgy, Baku: Maarif, 334 pages.

Khazar Journal of Science and Technology `Volume 9 №1 2025, 21-26
 DOI: 10.5782/2520-6133.2025.9.1.21

Investigation of Some Chemical Indicators in Okhchuchay River

Aiten Samadova
Ecological Chemistry Departament, Baku State University, Baku, Azerbaijan
Corresponding author: aytan.samad@gmail.com

Abstract
Assessing the environment in the liberated territories is crucial and relevant. In this context, rivers originating from neighboring areas in these regions are of particular importance. To organize the eco-chemical assessment of the Okhchuchay River, the dynamics of concentration changes along the water flow were studied in March. It was determined that during March, the levels of hardness, ammonium, and manganese ions in the Okhchuchay River were significantly above the permissible limits.
Keywords: anion, cation, metals, physicochemical parameters, Okhchuchay

Introduction

Monitoring of the liberated territories is extremely important. Since living organisms in these areas rely on river waters, continuous research is necessary (Hajiyeva, et al., 2019; Mammadov, et al., 2005). An excessive amount of any parameter in water can disrupt the ecosystem. Additionally, metals and various chemical parameters must be constantly monitored due to their impact on living organisms (Medvedev, et al., 2017; Moore, 1987; Mudry, 1997; Skalny, 1999). One of the key factors affecting the biosenosis is the pH interval. Therefore, this indicator is primarily analyzed during research, followed by an examination of its physicochemical properties (Teplaya, 2013; Avtsyn, 1991).

Materials and Methods

An Etrex 10 device was used to determine the sampling coordinates. Subsequently, the physicochemical parameters of the water samples were analyzed. The parameters examined included pH, dissolved oxygen, electrical conductivity, hardness, Cl^-, SO_4^{2-}, NH_4^+, NO_2^-, NO_3^-, Cu, Fe, Mn, Mo, Pb, Zn, Co, and Ni (GOST 24481-80, 1986). The elemental composition

was determined using an atomic absorption spectrometer, while anions were analyzed using a spectrometer (Lurye, 1979; Korostilev, 1981).

Result

Considering that a river is a self-purifying system, we collected samples from the upper, middle, and lower reaches of the river. The sampling coordinates are provided in Table 1.

Table 1. Sampling Coordinates for Okchuchay

№	Name of area	Coordinates
1	Burunlu	$39^0$10'23.5" $46^0$30'39.8"
2	Shayifli	$39^0$07'19.1" $46^0$34'19.7"
3	Jahangirbayli	$39^0$02'43.1" $46^0$44'09.0"

The analyses were conducted throughout March, with samples taken in each ten-day period. The results are presented in Tables 2, 3, and 4.

Table 2. Analysis results of the water sample taken from Okchucay on 06.03.2024.

№	Name of component	Unit of measure-ment	Amount of components			MPC
			Okchuchay-Zangilan district			
			Burunlu village	Sayifli village	Jahangirbe yli village	
1	pH	–	7.9	8.0	7.8	6.5-8.5
2	Dissolved oxygen	mgO_2/l %	8.3 85.0	8.2 84.0	8.3 85.0	≥4.0
3	Electrical conductivity	µS/cm	1493	1448	1532	–
4	Hardness	mg-ekv/l	12.08	12.0	13.3	7.0
5	Cl^-	mg/l	16.3	15.9	18.4	350
6	SO_4^{2-}	mg/l	441.8	447.7	456.3	500
7	NH_4^+	mg/l	1.1	0.9	0.1	0.5
8	NO_2^-	mg/l	0.6	0.95	0.93	3.3
9	NO_3^-	mg/l	4.3	4.21	4.09	45.0
10	Cu	mkg/l	20.7	11.0	6.94	1000
11	Fe	mkg/l	28.0	69.1	61.7	300
12	Mn	mkg/l	348	323	313	100
13	Pb	mkg/l	0.401	0.158	0.150	30
14	Zn	mkg/l	37.1	38.8	40.0	1000

15	Co	mkg/l	4.15	5.55	4.97	100
16	Ni	mkg/l	2.29	<LOD	<LOD	100
17	Mo	mkg/l	242	247	209	250

As seen in Table 2, the analysis of water samples indicates that hardness levels in Okchuchay exceed the Maximum Allowable Concentration (MAC) by 1.7 times in Burunlu and Sayifli villages and by 1.9 times in Jahangirbayli village. The ammonium ion concentration is 2.2 times higher than the MAC in Burunlu, 1.8 times higher in Sayifli, and manganese levels exceed the MAC by 3.5 times in Burunlu, 3.2 times in Sayifli, and 3.1 times in Jahangirbayli. It is important to note that the Maximum Allowable Concentrations (MAC) for surface waters were established by the State Committee for Ecology and Nature Use Control of the Republic of Azerbaijan under Order No. 01 dated January 4, 1994, as part of the "Regulations on the Protection of Surface Waters from Pollution by Wastewater."

Table 3. The results of the analysis of the water sample taken from Oxçuçay on 13.03.2024.

№	Name of component	Unit of measure-ment	Amount of components			Permissible viscosity limits
			Okchuchay-Zangilan district			
			Burunlu village	Sayifli village	Jahangirbeyli village	
1	pH	—	6.9	7.3	7.2	6.5-8.5
2	Dissolved oxygen	mgO_2/l %	9.7 98.0	9.7 99.0	9.5 97.0	≥4.0
3	Electrical conductivity	µS/cm	1131	1632	1628	—
4	Hardness	mg-ekv/l	9.4	14.0	14.3	7.0
5	Cl^-	mg/l	18.1	18.1	17.4	350
6	SO_4^{2-}	mg/l	340.2	430.5	412.3	500
7	NH_4^+	mg/l	0.62	0	0	0.5
8	NO_2^-	mg/l	0.7	0.72	0.8	3.3
9	NO_3^-	mg/l	4.65	4.91	5.13	45.0
10	Cu	mkg/l	13.0	9.76	11.4	1000
11	Fe	mkg/l	88.6	77.9	84.4	300
12	Mn	mkg/l	180.0	111.0	109.0	100
13	Pb	mkg/l	0.131	0.870	0.608	30
14	Zn	mkg/l	36.4	31.1	38.5	1000
15	Co	mkg/l	3.67	4.34	3.47	100
16	Ni	mkg/l	0.0269	<LOD	<LOD	100
17	Mo	mkg/l	104.0	177.0	173.0	250

On 13.03.2024, the hardness level in the water exceeded the permissible concentration limit by 1.3 times in Burunlu, 2 times in Shayifli, and 2.04 times in Jahangirbayli. The ammonium parameter exceeded the permissible concentration limit by 1.24 times in Burunlu. Manganese exceeded the permissible concentration limit by 1.8 times in Burunlu, 1.11 times in Sayifli, and 10.9 times in Jahangirbayli.
Considering the flow of the river, the third sample was taken again on the 28th of the month. The results are presented in Table 4.

Table 4. Results of the analysis of the water sample taken from Okchuchay on 28.03.2024.

№	Name of components	Unit of measurement	Amount of components			MPC
			Okchuchay-Zangilan district			
			Burunlu village	Shayifli village	Jahangirbayli village	
1	pH	—	7.5	7.3	7.1	6.5-8.5
2	Dissolved oxygen	mgO_2/l %	9.2 94.0	9.0 93.0	9.1 92.0	≥4.0
3	Electrical conductivity	µS/cm	609	614	615	—
4	Hardness	mg-ekv/l	5.32	5.4	5.41	7.0
5	Cl^-	mg/l	9.4	10.9	11.0	350
6	SO_4^{2-}	mg/l	150.87	152.44	153.1	500
7	NH_4^+	mg/l	**0.63**	**0.52**	**0.52**	0.5
8	NO_2^-	mg/l	0.04	0.21	0.23	3.3
9	NO_3^-	mg/l	4.13	4.61	4.63	45.0
10	Cu	mkg/l	16.1	23.0	22.2	1000
11	Fe	mkg/l	**368**	**357.0**	**350.0**	300
12	Mn	mkg/l	33.8	31.3	32.4	100
13	Pb	mkg/l	0.981	0.312	0.306	30
14	Zn	mkg/l	10.3	8.70	10.1	1000
15	Co	mkg/l	<LOD	<LOD	<LOD	100
16	Ni	mkg/l	71.8	82.1	80.1	250

As shown in Table 4, according to the analyses of the water samples, ammonium ions in Okchuchay were 1.3 times higher in Burunlu village, 1.02 times higher in Sayifli and Jahangirbayli villages, and iron in Okchuchay was 1.2 times higher than the permissible limits in Burunlu, Sayifli, and Jahangirbayli villages.
In the beginning of March, the hardness level in the Burunlu village area was 12.08 mg-equiv/l. In the second ten-day period of the month, it decreased to

9.4 mg-equiv/l, and by the end of the month, it further dropped to 5.32 mg-equiv/l. The norm for hardness is 7 mg-equiv/l. Considering the river's self-regulating property, the hardness was 1.73 and 1.34 times above the norm in the first and second periods, respectively. At the same time, the ammonium ion exceeded the norm on all three dates. Specifically, on March 6th, it was 1.1 mg/l; on March 13th, it was 0.62 mg/l; and on March 28th, it was 0.63 mg/l, which means it exceeded the norm by up to 2.2 times. The manganese ion, which was 348 μg/l at the beginning of the month, dropped to 180 μg/l in the second ten-day period. However, despite this decrease, its levels were still 3.48 times and 1.8 times above the norm, which is considered a significant amount. Given that the river is 82 km long within Azerbaijan, if the concentration limit were somewhat lower over such a distance, the river could potentially be self-cleaning. However, the high levels of such critical parameters affect the integrity of the ecosystem (Vorobyov, 2007; Israel, 979; Onishchenko, 2002). Water with high hardness, when consumed over a long period, can lead to the precipitation of calcium and magnesium protein compounds on the walls of the stomach and esophagus, which complicates peristalsis and disrupts the function of enzymes (Mudry, 2008). Additionally, frequent consumption of hard water can lead to dysbacteriosis. High levels of ammonium in the blood can lead to severe pathology. Consuming water with high ammonium ion levels can result in serious lung diseases and genetic enzyme disorders. Cases of consciousness impairment are also reported. The excess of manganese disrupts plant development and affects metabolic processes in animals (Shachneva, 2012; Filov, 2004; Davidova, 1991). It also makes the central nervous system highly sensitive. When the permissible amount is exceeded, manganese-induced Parkinson's syndrome damage is observed in the nervous system. It affects the reproductive processes of living organisms. Additionally, consuming water with high manganese levels causes intoxication in humans, leading to memory impairment and disruptions in the lymphatic system (Hajiyeva *et al.*, 2021; Hajiyeva, *et al.*, 2019).

References

Avtsyn, A.P. (1991) Human microelementoses. A.P. Avtsyn, A.A. Zhavoronkov, M.A. Rish, L.S.Strochkova. M.: Medicine. P.496.

Davidova, S.L. (1991). About the toxicity of metal ions. Series "Chemistry" №3, 243.

Filov, V.A. (2004) Chemical pollutants of the environmental, toxicology and information issues. Ros.chem. journal. t. 48. № 2, p.4-8.

GOST 24481-80. (1986) Drinking water. Taken of sample: M.: State Committee of the USSR on standards, p.4.

Hajiyeva, S.R., et al. (2019). Fundamentals of ecotoxicology., p.123-136

Hajiyeva, S.R., et al. (2019). Practicum of ecologycal monitoring., 140.

Hajiyeva, S.R., et al. (2021). Chemical ecotoxicology, 288.

Israel, Yu. A. (1979). "Ecology and control of the state of the natural environment", 1979

Korostilev, P.P. (1981) Preparation of solutions for chemical and analytical works. -M.: Nauka. p.202.

Lurye, Yu.Yu. (1979) Handbook of analytical chemistry. M.: Chemistry. p.480. (in Russian)

Mammadov G., et al. (2005). Ecology and environmental protection, p.880.

Medvedev, I.F., et al. (2017) Heavy metals in ecosystem. Saratov. Rakursc, p.178.

Moore, JW, et al. (1987). Heavy metals in natural waters. M.:Mir, p.297

Mudry, I.V. (1997) Heavy metals in the soil-plant-human system. Hygiene and sanitation. – Moscow, № 1, p.14-16.

Mudry, I.V. (2008) The impact of chemical contamination of soil on public health. Hygiene and Sanitation, №4, p.32-37.

Onishchenko, G.G. (2002) Fundamentals of assessing the risk to public health when exposed to chemicals polluting the environment. M.: Research Institute of ECh and GOS, Bibliography: p.305-324.

Shachneva, E.U. (2012). Impact of heavy toxic metals on the environment. Scientific potential of regions for the service of modernization. 2(3), 127-134.

Skalny, A.V. (1999). Microlementoses in humans (diagnosis and treatment): Practical manual for doctors and students of medical universities.M.: Printhouse, Nauchniy mir, p95. (Series "School of Biotic Medicine"). Bibliography: p. 92-93.

Teplaya, G.A. (2013) Heavy metals as a factor in environmental pollution. Astrakhan Bulletin of Environmental Education. №1(23) p. 182-192.

Vorobyov, D.V. (2007) Biogenic migration of metals in soils, water and plants of the Lower Volga. Vorobyov D.V., Andrianov V.A., Osipov B.E. Collection of articles (Authors: V.P. Pilipenko and A.V. Fedotova). Astrakhan. Publishing House of Astrakhan State University, part II.2007. 16-22.

Khazar Journal of Science and Technology `Volume 9 №1 2025, 27-31

DOI: 10.5782/2520-6133.2025.9.1.27

Highly Efficient Removal of Oil from Wastewater by Bio-nanoadsorbents

[1]U.N.Abdullayeva, [1]S.R.Hajiyeva, [1,2]F.V.Hajiyeva

[1]Ecological Chemistry Departament, Baku State University, Baku, Azerbaijan
[2]Western Caspian University, Baku, Istiglaliyyat 31, AZ 1001, Baku, Azerbaijan
Corresponding author: ulkar9522@gmail.com

Abstract
In our research, we used pomegranate peels and hazelnut shells as plant of origin to clean oil-contaminated water. The main objective of the work was to determine the optimal conditions for oil absorption by pomegranate and hazelnut shell bio-adsorbents, pomegranate peels and hazelnut shells, and Fe_3O_4 bio-nanoadsorbents. The effects of bioadsorbent and bio-nanoadsorbents, nanoparticles, and oil concentration, temperature, and pH on oil adsorption were studied to find the optimal conditions.

Key words: pomegranate peels, hazelnut shells, plant of origin, bio-nanoadsorbents, absorption

Introduction
Oil pollution in the environment is considered toxic and dangerous to the human body. Many methods are used to clean water from oil and oil product spills in the environment (Ferrero, 2007). Removing oil from oil-contaminated waters without harming the environment is considered a significant challenge for the oil industry. Plant-based adsorbents, which are considered environmentally friendly products, were used to clean up the oil from water (Nenkova, *et al*., 2004). The transformation of plant of origin into a valuable adsorbent with high adsorption capacity is presented as a new method for cleaning agricultural waste from the environment.
A new type of adsorbent (bio-nanoadsorbent) with nanoparticles has been synthesized to increase the effectiveness of plant of origin for oil removal from water. To increase the absorbency of pomegranate peel and hazelnut shell, magnetite nanoparticles were impregnated onto the surface of the plant waste we used. Fe_3O_4 nanoparticles, a magnetite nanoparticle, were used due to their high surface-to-volume ratio and their ability to absorb and react. Fe_3O_4 magnetite nanoparticles were used during the synthesis of the bio-nanosorbent (Bhatnagar and Sillanpää, 2010).

The oil sorption capacity of hazelnut shells, a plant-based biosorbent, was determined to be 61.25%, and the oil sorption capacity of pomegranate shells was determined to be 71.5%.

The new bio-nanoadsorbent synthesized based on hazelnut shell + Fe_3O_4 nanoparticles has an oil absorption capacity of approximately 92.5%, while the pomegranate shell + Fe_3O_4 bio-nansorbent has an oil absorption capacity of approximately 100%, depending on time.

Materials and Methods

Firstly, pomegranate peels and hazelnut shells are dried in a muffle furnace at 60^0C for 24 hours, then crushed.

Then, Fe_3O_4 nanoparticles are synthesized to increase sorption. Fe_3O_4magnetic nanoparticles were synthesized by co-precipitation of Fe^{3+} and Fe^{2+} ions in the ratio of (3:2) with ammonium solution in the presence of polyethylene glycol (Ravikumar, *et al*., 2017).

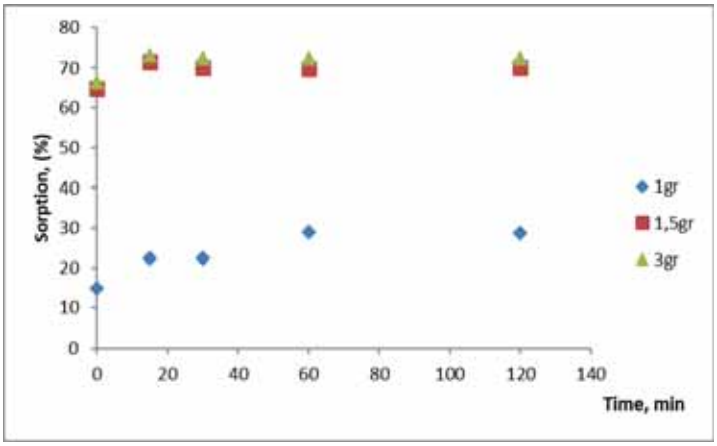

Figure 1. Time dependence of oil sorption of pomegranate peel biosorbent

The synthesized superparamagnetic Fe_3O_4 nanoparticles are then mixed with 1 ml of NH_4OH solution and impregnated onto pomegranate peels and hazelnut shells for 1 hour, thereby synthesizing a new type of bio-nanoadsorbents (Yang, *et al*., 2020).

After synthesis of biosorbent and bio-nanosorbent, oil purification process was carried out.

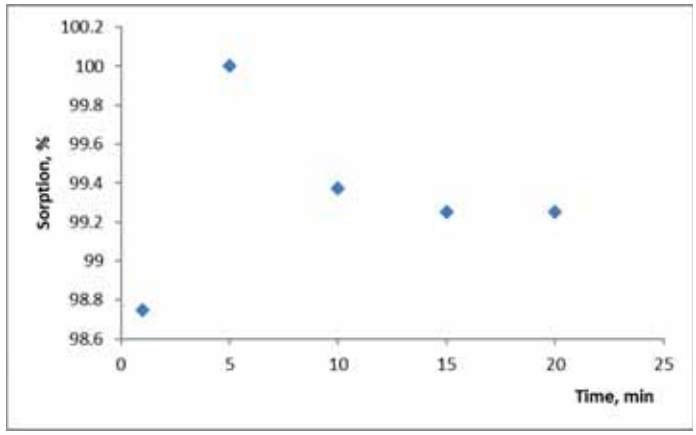

Figure 2. Time dependence of the amount of pomegranate peel+Fe_3O_4 bionanosorbent in oil sorption

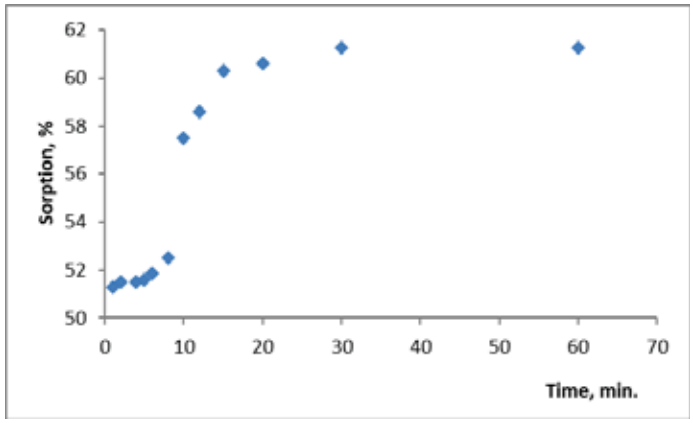

Figure 3. Time dependence of oil sorption of po hazelnut shell biosorbent

Oil-contaminated water was obtained by mixing 10 ml of oil in 100 ml of water (Ajji and Al-Ghouti, 2021). Bio-nanoadsorbent synthesized based on pomegranate peel, hazelnut peel, pomegranate peel+Fe_3O_4 nanoparticles, and bio-nanoadsorbent synthesized based on hazelnut peel+Fe_3O_4 nanoparticles were added to the obtained oil-contaminated water, respectively, and the sorption process was carried out. In the sorption process, the time dependence experiment was initially carried out (Shartooh, *et al*., 2018). The time dependence experiment was carried out in 1, 2, 4, 6, 10, 12, 15, 20, 30, 60 minutes According to the time-dependent experiment of the sorption process for biosorbent and bio-nanoadsorbent, pomegranate peel adsorbs 71.5% of oil in 15 minutes, bio-nanoadsorbent synthesized

based on pomegranate peel + Fe_3O_4 nanoparticles adsorbs approximately 100% in 1 minute, hazelnut peel adsorbs 61.25% of oil in 30 minutes, and bio-nanoadsorbent synthesized based on hazelnut peel + Fe_3O_4 nanoparticles adsorbs 92.5% of oil in 12 minutes. Based on the dependence graph of the time dependence of pomegranate peel and hazelnut peel, as well as the nano-composite of each, it can be clearly determined that the bio-nanoadsorbent synthesized on the basis of pomegranate peel + Fe_3O_4 nanoparticles has a greater oil absorption capacity than other biosorbents and bionanosorbents (Feumba *et al*., 2016; Bhatnagar, *et al*. 2010) .

Figure 1 shows that the absorption of oil based on pomegranate peel was determined by the plant-based adsorbent, with 29% of the oil absorbed by 1 gram of pomegranate peel in 1 hour, 71.5% in 1.5 grams of pomegranate peel in 15 minutes, and 73.25% in 3 grams of pomegranate peel in 15 minutes.

Figure 2 shows that the pomegranate peel bio-nanoadsorbent has the ability to absorb approximately 100% of the oil within 5 minutes.

If we look at the time dependence graph of the oil adsorption of the hazelnut shell, it is determined that the pure vegetable hazelnut shell has the ability to absorb 61.25% oil in 30 minutes (Fig.3.).

Figure 1 shows that the based on the experimental results, it is determined that the bio-nanoadsorbent synthesized based on hazelnut shell + Fe_3O_4 nanoparticles has the ability to adsorb 92.5% of oil within 12 minutes.

Result

A new plant-based sorbent and bio-nanoadsorbent were synthesized for the purification of water contaminated with oil and oil products. The time of oil adsorption of the biosorbent and bio-nanoadsorbent was determined. It is possible to prevent oil pollution from water using pomegranate peels and hazelnut shells, which are plant-based waste. In our research, it was determined that pomegranate peels and hazelnut shells have the ability to adsorb oil from the aquatic environment by reusing them. Our research is based on the principle of low-waste and waste-free technology.

As a result, the oil sorption capacity of hazelnut shells is 61.25%, the oil sorption capacity of pomegranate shells is 71.5%, the new bio-nanoadsorbent synthesized on the basis of hazelnut shell + Fe_3O_4 nanoparticles has an oil absorption capacity of approximately 92.5%, and the pomegranate shell + Fe_3O_4 bionansorbent has an oil absorption capacity of approximately 100%, depending on time.

References

Al-Ajji, M.A. & Al-Ghouti M.A. (2021). Novel insights into the nanoadsorption mechanisms of crystal violet using nano-hazelnut shell from aqueous solution. J. Water Process Eng. 44, 102354.

Bhatnagar, A. & Sillanpää, M. (2010). Utilization of agro-industrial and municipal waste materials as potential adsorbents for water treatment—A review. Chem. Eng. J., 157, 277–296.

Ferrero, F. (2007). Dye removal by low cost adsorbents: Hazelnut shells in comparison with wood sawdust. J. Hazard. Mater. 142, 144–152.

Feumba, D.R., Ashwini, R.P., & Ragu, S.M. (2016). Chemical composition of some selected fruit peels, European Journal of Food Science and Technology. 4(4): 12-21.

Nenkova, S., Herzog, M., Gancheva, V. & Garvanska, R. (2004). Fibrous wood sorbent for eliminating oil pollution, AUTEX Research Journal. 4(3): 157-163.

Ravikumar, S., Ibrahim, H. & Al Zubaidi, I. (2017). Separation of oil from produced water by adsorption on pinecone powder, Williston Basin Petroleum Conference, Evraz Place, Regina, Saskatchewan, Canada.

Shartooh, S. M., Al-Azzawi, M.N.A., Al-Hiyaly, S.A.K. (2018). Pomegranate Peels as Biosorbent Material to Remove Heavy Metal Ions from Industerial Wastewater, Iraqi Journal of Science.

Yang, W., Wang, J., Shi, X., Tang, H., Wang, X., Wang, Sh., Zhang, W. & Lu, J. (2020). Preferential Nitrate Removal from Water Using a New Recyclable Polystyrene Adsorbent Functionalized with Triethylamine Groups. Ind. Eng. Chem. Res. 59, 5194–5201.

Khazar Journal of Science and Technology `Volume 9 №1 2025, 32-46
 DOI: 10.5782/2520-6133.2025.9.1.32

A survey of Web Assembly Runtime Ecosystem

Vugar Hasanov, Sallar Khan, Tania Malik, Khalid Hasanov
Faculty of Engineering and Applied Sciences, Khazar University, Azerbaijan
School of Informatics and Cybersecurity, Technological University Dublin, Ireland
Corresponding author: vugar.hasanov96@gmail.com

Abstract
WebAssembly is a secure, portable, low-level binary code format that offers efficient execution and compact representation. With the intro- duction of the WebAssembly System Interface, Wasm is expanding beyond its original role as a browser-only technology, finding applications in diverse fields such as generative AI, serverless AI, edge computing, cloud computing, and high-performance computing. Despite the existence of numerous Wasm run- time ecosystems, there is currently no comprehensive overview or taxonomy of these state-of-the-art runtimes and their ecosystems. This paper aims to fill that gap by providing a detailed taxonomy of Wasm runtime ecosystems, ex- amining runtime characteristics and classifying modern Wasm runtimes within this framework.
Keywords: WebAssembly, Wasm, WASI, Wasm Runtimes

Introduction
WebAssembly (Wasm) is a safe, portable, low-level binary-code format designed for efficient execution and compact representation. Introduced in 2015 as an al- ternative to JavaScript for web browser-based applications (WebAssembly Contributors, 2015). Wasm serves as a cross-platform compilation target for languages traditionally not executed on the web, such as C/C++ (WebAssembly Working Group, 2022). It has been developed as an open standard by the World Wide Web Consortium (W3C), and all major browsers support it (McConnell, 2017). In particular, most modern web browsers enable the loading of Wasm modules through JavaScript, facilitating nearly native performance in web application vir- tual machines. Since Wasm was originally designed for web browsers, it lacked a system interface targeting POSIX environments, which would enable the execu- tion of Wasm modules on these environments as part of its original specification (Andreas, et al., 2017). To address this, the WebAssembly System Interface (WASI) specification was designed (WebAssembly Community Group, 2021). With the introduction of WASI, WebAssembly has begun to tran- scend its browser-only limitations, evolving from a technology exclusively

used in browsers to one that spans various application areas, including generative AI, serverless computing, edge computing, cloud computing, and high-performance computing. WASI provides a standardized set of system interfaces for WebAssem- bly modules, enabling them to interact with the operating system in a secure and portable manner. Its sandbox execution environment and portability also make Wasm an ideal candidate for non-web use cases. The environment in which We- bAssembly code executes is called Wasm runtime. These runtimes are crucial because they parse and execute the compiled WebAssembly modules, allowing them to run as efficiently and securely as possible.

A large number of Wasm runtimes have been developed over the past couple of years, and Wasm runtimes have started to be incorporated within or extend higher-level system software. While the usage of Wasm and Wasm runtimes within web browsers are still dominant, the focus of this work is to categorize WebAssem- bly runtimes which are in use outside web browsers. It is worth emphasising that we intentionally do not cover Wasm runtimes that are not actively maintained anymore and do not have commit histories in their GitHub repositories within the last one year.

Unlike previous works in this domain, this paper does not focus solely on stan- dalone Wasm runtimes. Instead, it also includes new emerging wrapper runtimes that are built on top of a standalone runtime and extend it with new functionalities for distributed hosts and server-side application development. While it could be argued that wrapper runtimes are not fundamentally WebAssembly runtimes, the wrapper runtimes examined in this work are specifically designed for WebAssem- bly. They extend a single host WebAssembly runtime with additional layers of security, a distributed application platform, an observability layer, RPC (remote procedure call) capabilities, channel-based message passing, massive concurrency control with their own runtime scheduler, and more. Therefore, these wrapper runtimes deserve to be mentioned and included within a broader classification of WebAssembly runtimes.

For the purpose of this work, we define a WebAssembly runtime as follows: A WebAssembly runtime is a software platform that features a virtual machine executing the WebAssembly instruction set according to the WebAssembly specification. Execution can be managed directly by the runtime itself, or, in more complex designs, it may rely on another We- bAssembly runtime underneath while adding additional functionalities on top.

The Wasm ecosystem and standards are evolving rapidly, which naturally forces Wasm runtimes to catch up with the new developments. Not every Wasm run- time implements and support all Wasm or WASI standards. For

instance, some runtimes, such as Wasmer (2024) and Wasmedge (2024) implement the proposal (Bytcode Alliance-a, 2024) to add garbage collection (GC) support to WebAssembly, while Wasmtime (Bytcode Alliance-b, 2024) does not have a stable implementation yet. Similarly, APIs and integrations provided by different runtimes are different, some of them provides a wide range of program- ming language SDKs, while others are designed with a specific language in mind.

The landscape of Wasm runtimes, already rich with diversity, is further expanded by the emergence of advanced wrapper runtimes, like Lunatic (Lunatic Inc, 2023) and wasmCloud (WasmCloud LLC, 2024). Both of these runtimes rely on Wasmtime as their foundation, offering higher-level abstractions to facilitate the creation of distributed applica- tions utilizing WebAssembly.

There have been some recent efforts to provide a taxonomy of WebAssembly runtimes and Wasm ecosystem. While the research in (Zhang, et al., 2024) does a thorough study on this front, the focus of that work is to study and classify the previous academic research efforts in the Wasm runtime implementations. However, there is a notable absence of an updated and thorough classification of more recent Wasm runtimes and higher level runtimes that are based on standalone Wasm runtimes. This absence leaves researchers and developers interested in WebAssembly runtimes without a clear understanding of the alternatives to traditional non-WebAssembly technologies. In this study, we aim to fill this gap by presenting a taxonomy of standalone runtimes, as well as, new emerging higher level wrapper and inte- grated runtimes; We validate the usefulness of this taxonomy by applying it to categorize several WebAssembly runtimes. While these runtimes vary in maturity and stability, they collectively offer insight into the landscape of WebAssembly runtimes in use. Broadly, we define each WebAssembly runtime as consisting of two main components: a programming interface (API) and a runtime system. The API serves as the interface between the environment and the programmer, while the runtime system comprises the underlying implementation mechanisms. Additionally, the runtime itself may include various subcomponents to fulfill its functionalities. In this study, we concentrate on the runtime systems, reserving the classification of APIs for future research.

1. WebAssembly Runtimes

WebAssembly is a binary instruction format that runs within a stack-based virtual machine (VM). The stack-based VM records operand values and control constructs. In addition, it provides an abstract store for the global

state. The stack-based virtual machines are implemented by different WebAssembly run- times.

In this section, we classify existing WebAssembly runtimes into five broad cat- egories: type, architecture, platform, compilation mode, and finally execution environment.

1.1. WebAssembly Runtime Types

The first classification item in this category is the type of the Wasm runtime. Not all the Wasm runtimes are designed the same and there are fundamental differences in the way they have been implemented and the way they can be used to build applications. With this in mind, we classify the state-of-the-art WebAssembly runtimes into standalone, integrated, and wrapper runtimes. It is important to note that this classification is one of the primary distinction between this work and previous research in this field.

(1) Standalone WebAssembly Runtimes

The standalone Wasm runtimes have zero or less dependencies and usually do not assume the existence of other runtimes to execute Wasm binaries. This makes them ideal for environments where a lightweight and self- contained execution environment is necessary.

(2) Integrated Webassembly Runtimes

Unlike the standalone Wasm runtimes, the integrated runtimes are de- signed in a way that they cannot run on their own and need to be ex- ecuted within the context of another runtime. The another runtime in this context is not necessarily a runtime dedicated for WebAssembly. For instance, there are integrated Wasm runtimes based on JDK or Go pro- gramming language runtimes and cannot operate on their own without the corresponding language runtimes.

(3) Webassembly Wrapper Runtimes

A wrapper runtime is based on a standalone Wasm runtime and extends it with different features, such as distributed application development, net- working, process supervision, hot reloading, and so on. This approach helps to abstract Wasm runtimes further and enables their usage beyond a single host. Wrapper runtimes are typically used to simplify the de- velopment and deployment of complex applications that need to operate across multiple environments or require enhanced functionalities and in- teractions.

Unfortunately, the industry terminology for standalone Wasm runtimes is convoluted and inconsistent. For example, the state-of-the-art server- side WebAssembly runtime, Spin (Fermyon Technologies-a, 2024), is variously described as an ”open source developer tool for building and running serverless applications pow- ered by WebAssembly” and as ”a framework for building, deploying, and running fast, secure, and composable cloud microservices with WebAssem- bly.” In scientific research, it is crucial to

clearly differentiate between terms like ”developer tool” and ”framework.” A closer examination of Spin’s features reveals that such a complex system merits being classified as a runtime in its own right. Indeed, the core developers of the Spin project refer to it as a runtime for server-side WebAssembly in GitHub is- sue discussions (Spin (Fermyon Technologies-b, 2024). Therefore, we hope that by introducing the term ”We- bAssembly Wrapper Runtime” and classifying corresponding runtimes as such, this work will help standardize terminology in both the industry and the research community.

1.2. Architecture

As the name suggests, this feature covers CPU architectures supported by Wasm runtimes. We broadly classify the supported architectures into 32-bit and 64-bit systems. The rationale to group Wasm runtimes into these two categories is that, if a runtime supports a specific 32-bit architecture, it usually easily be extended to support another 32-bit architecture. 32-bit architectures usually used in embedded-processors and constrained edge devices.

1.3. Platform

This criteria covers platforms supported by different Wasm runtimes. The list of platforms classified are Android, FreeBSD, iOS, Linux, macOS, Windows. In addition, we broadly cover real-time and embedded operating systems platforms under this category.

1.4. Compilation Mode

WebAssembly runtimes can operate in different compilation modes: Ahead-Of- Time (AoT), Just-In-Time (JIT), and Interpreted.

(1) Ahead-of-Time Compilation(AoT)

Whether the runtime supports ahead-of-time compilation of Webassembly programs into a Wasm binary before execution of the program at a build-time. AoT compilation usually reduces the amount of work needed to be performed at run time. The benefits of AoT are faster startup times and predictable performance.

(2) Interpreted

Whether the runtime can simply interpret the Wasm code. The main benefit of this mode is that, it simplifies implementation and allows for immediate execution without the need for compilation. It generally has slower execution speed compared to AoT and JIT.

(3) Just-in-Time compilation (JIT)

Whether the runtime supports just-in-time (JIT) compilation. In the JIT compilation mode the Wasm program is compiled during execution of the program at run time, rather than before its execution. The benefit of JIT is

potentially better optimization based on runtime information. However, it may introduce overhead due to the compilation step during execution.

1.5. Execution Environment

The execution environment of a Wasm runtime is a criteria to indicate whether the runtime is designed to run on a single host only or on a distributed set of nodes.

(1) Single host

Whether the Wasm runtime is designed for a single host

(2) Distributed

Whether the Wasm runtime can run on a distributed set of nodes With these definitions in place, in this work, we provide a set of characterizing features for Webassembly runtimes which encompasses all relevant aspects while remaining as compact as possible; Figure 1 presents our Wasm runtime taxonomy.

2. WebAssembly Runtime Classification

In the previous section, we defined categories for Wasm runtimes. However, we have not classified existing runtimes into those categories. That is the scope of this section where we classify each of the state-of-the-art Wasm runtime we studied.

2.1. Runtime Types

(1) Standalone Runtimes

The leading examples of standalone Wasm runtimes include Wasmtime, Wasmer, Wasmi, Wasm3, WasmEdge, and Wazero. While these runtimes differ in the way they have been implemented and the features they all provide, they all have a common graund; these runtimes are implemented

(2) Integrated Runtimes

A prominent example for integrated Wasm runtimes is Chicory (Chicory Runtime, 2024), which is a JVM native WebAssembly runtime. Chicory can run Wasm binaries on any platform where a JVM can run.

GraalWASM (Oracle, 2024) is another example of an integrated Wasm runtime that is built on top of GraalVM. It can interpret and compile Wasm pro- grams in the binary format, or be embedded into other programs.

Wazero (2024) is another actively maintained Wasm runtime and it is built on top of Go runtime. Wazero does not use shared libraries or libc, this means it can also be embedded into applications that do not use an oper- ating system.

(3) Wrapper Runtimes

Lunatic (2023) is a state-of-the-art wrapper runtime. It is written in Rust and uses Wasmtime to create processes as WebAssembly instances. It was inspired by Erlang and can be used to build highly-concurrent and distributed server side applications. The massive concurrency support is provided via the robust work stealing scheduler implementation in Tokio, Rust's asynchronous runtime.

Spin (Fermyon Technologies-a, 2024) is a server-side WebAssembly runtime built to run applications compiled to WebAssembly.

Another actively developed wrapper runtime is WasmCloud (2024) which is based on Wasmtime as well.

Wasmex (2024) is another actively developed wrapper runtime that uses Wasmtime underneath. It enables the execution of Wasm binaries within Elixir programs through the utilization of the Wasmtime Rust library.

Extism (2024) is a lightweight framework for building Wasm applications and running them both on the browsers and servers, including the edge, command line interfaces, the internet of things. While Extism can be seen as a feature full framework providing support for persistent memory variables, secure and host-controlled HTTP, runtime limiters and timers, simpler host function linking, and so forth, it can also be classified as a Wasm wrapper runtime. As a matter of fact, it provides its own runtime implemented as a Rust crate and uses Wasmtime underneath to extend it with the mentioned functionalities. Moreover, Extism can use different standalone Wasm runtimes underneath. Namely, it uses Wasmtime for host SDKs, and Wazero for Go based applications. Also, for the browser runtimes, it can use V8 in Node/Deno, and JSC for Bun. Therefore, it very well belongs to our definition of wrapper runtime.

MPIWasm (Mohak, et al., 2023) is an academic wrapper runtime based on Wasmer and allows to execute high-performance MPI applications compiled to Wasm binaries on distributed memory platforms. The runtime supports the ex- ecution of MPI-2.2 standard applications written in C/C++.

2.2. Supported Architectures and Platforms

WebAssembly runtimes have evolved to support a wide range of architectures and platforms, enabling developers to run Wasm code efficiently across different environments. They offer robust support for various operating systems, such as Linux, Windows, macOS, and more, as well as compatibility with architectures like x86, ARM, and RISC-V. Below section categorizes various Wasm runtimes according to the platforms and architectures they support.

(1) Chicory

Chicory runtime is written purely in Java, supports running on any architecture and platform that the underlying JVM runtime supports. It does not rely on platform-specific native dependencies, making it highly portable and suitable for various environments.

(2) Extism

Architecture: x64, aarch64, x86 Platform: Windows, Linux, MacOS

(3) Lunatic

Architecture: X86-64, aarch64 Platform: Windows, Linux, MacOS

(4) WAMR

Architecture: X86-64, X86-32, ARM, AArch64, RISCV64, RISCV32

Platform: Windows, Linux, MacOS, Android

(5) Wasmedge

Architecture: X86-64, AArch64, RISCV64, Raspberry Pi Platform: Windows, Linux, MacOS, Android

(6) Wasmtime

Architecture: X86-64, AArch64, RISCV64, s390x Platform: Windows x86-64, Linux x86-64, MacOS x86-64

Wasmtime uses cranelift code generator to compile wasm binary into na- tive machine code, and cranelift only supports 64 bits platforms. Due to this, no 32 bit platform is supported by wasmtime yet.

(7) Wasm3

Architecture: X86-64, X86-32, ARM, RISCV64, RISCV32, Raspberry Pi Platform: Windows, Linux, MacOS, FreeBSD, Android, IOS

(8) Wasmer

Architecture: X86-64,X86-32, ARM64, RISCV64, M1

Platform: Windows, Linux, MacOS, Android, IOS

(9) wasmCloud

Architecture: x86-64, aarch64 (ARM64)

Platform: Windows, Linux, MacOS

(10) Spin

Architecture: X86-64, ARM64 Platform: Windows, Linux, MacOS

(11) Wazero

Wazero is similar to Chicory runtime as it doesn’t have a built-in platform dependency in mind. It is written in Go programming language and can be run in any environment supported by Go.

Based on this information we can summarise this section that, Wasmtime, and the runtimes that are built on top of Wasmtime do not support 32-bit architec- tures. Wasmtime uses Cranelift as its compiler backend. While Cranelift supports various architectures, its primary focus and optimizations are directed towards 64- bit systems. The rest of the runtimes provide a 32-

bit architecture support to some extent. 32-bit architectures are often used in embedded processors or constrained edge devices due to their lower power consumption and cost. The integrated run- times, such as Chicory and Wazero, provide 32-bit architecture support via their underlying non-Wasm runtimes, namely, JDK and the Go runtimes respectively.

2.3. Compilation Mode

In Section 2.4 we reviewed different compilation modes. In this section we classify the existing Wasm runtimes within this taxonomy.

(1) Chicory

Compilation Mode: AOT and Interpreted

(2) GraalWASM

Compilation Mode: AOT and JIT

(3) Lunatic

Compilation Mode: JIT

(4) WAMR

Compilation Mode: Interpreted, AOT, and JIT

(5) Wasmedge

Compilation Mode: Interpreted and AOT

(6) Wasmtime

Compilation Mode: AOT and JIT

(7) Wasm3

Compilation Mode: Interpreted

(8) Wasmer

Compilation Mode: JIT and AOT

(9) Spin

Compilation Mode: same as Wasmtime since this is a wrapper runtime based on Wasmtime

(10) Wazero

Compilation Mode: AOT and Interpreted

2.4. Execution Environment

As previously mentioned, the execution environment of a Wasm runtime refers to whether it is designed to operate solely on a single host or across a distributed network of nodes. Most of the leading-edge runtimes fall into the first category, focusing on single-host operations. However, newer, higher-level wrapper run- times built on top of these foundational runtimes are increasingly designed with distributed node environments in mind.

(1) Single Host Wasm Runtimes

GraalWASM, Extism, Wasmex, WAMR, Wasmedge, Wasmtime, Wasm3,

Wasmer, Wazero, Spin

(2) Distributed Host Wasm Runtimes

Lunatic, MPIWasm, wasmCloud, Spin

3. Related Work

There are several survey papers related to WebAssembly that offer a broad and inclusive perspective on Wasm and provide comprehensive insights into its scope and applications. These surveys primarily focus on Wasm runtimes in general and explore their respective use cases. However, as the field, technology, and APIs are evolving very rapidly, there remains a gap in systematic research that offers an exhaustive categorization of the standard Wasm runtimes and APIs currently available. Our paper addresses these gaps, presenting aspects which are not covered in the existing literature.

Early work on the adaptation of Wasm to enhance the security of IoT systems has been explored in survey (Radovici, et al., 2018). The authors proposed that Wasm can be in- tegrated as part of a solution to improve the security of IoT by running verified bytecode in an isolated framework. This survey highlights Wasm potential as a foundational technology in developing robust security frameworks for IoT devices. In another early study (Jangda, et al., 2019) make an effort to comprehend how effectively Wasm binaries work. The research, however, is restricted to web browsers only and thus does not offer enough information about standalone runtimes.

The work of (Spies and Mock, 2021) is the first one that evaluates Wasm runtimes performance in non-web environments. The study conducts performance tests across five Wasm runtimes, including standalone and those integrated within traditional software systems in three non-web environments: desktop, server, and IoT device. The work of (Wang, et al., 2018) systemically characterizes and thoroughly analyzes major edge Wasm runtimes for the first time, highlighting their suitability based on extensive appli- cation scenarios and performance metrics. The work demonstrates that different runtimes fit different application scenarios. However, the scope of this work is limited to edge Wasm runtimes and doesn't provide a broader categorization of these runtimes across other potential environments.

Wang addresses the gap in previous studies by conducting a thorough char- acterization study of standalone Wasm runtimes. His work in (Wenwen, 2022) provides a detailed analysis of the standard Wasm runtimes. However, only the five most common independent Wasm runtimes are covered in this research. The study in (Kakati and Brorsson, 2023) provides a extensive review on how Wasm is applied outside traditional web contexts, specifically in edge and cloud computing environments. The authors reviewed different Wasm runtimes, compared their features and suitability for specific use cases, and identified research gaps and future directions for Wasm ex- pansion into more diverse computing environments. However, they mainly cover Wasm runtimes in the edge-cloud continuum.

The study in (Ray, 2023) provides an overview of Wasm evolution, reviews relevant development tools and runtimes, illustrates real-world applications,

and outlines both current challenges and future prospects for Wasm within IoT domain. How- ever, similar to other works in this domain, this study does not specifically focus on Wasm runtimes and APIs, but instead provides a broad overview of different Wasm runtimes and Wasm ecosystem in general with respect to IoT. A most re- cent survey on research on WebAssembly runtimes was presented in (Zhang, et al., 2024). This survey provides an extensive overview of Wasm runtimes, discussing research cov- ered in 98 articles on the subject. It explores Wasm runtime research from both internal perspectives (design, testing, analysis) and external applications across various domains. The paper also highlights the rapid evolution of Wasm technologies and proposes future research directions. This survey does a good job surveying different Wasm runtimes, however, their focus is to survey the existing research papers on Wasm runtimes and discuss the research focus of each paper, rather than classifying the state-of-the-art runtimes or their APIs.

4. Conclusion

The expansion of WebAssembly (Wasm) beyond its initial role as a browser-only technology into areas such as generative AI, serverless AI, edge computing, cloud computing, and high-performance computing has created a diverse ecosys- tem of Wasm runtimes. This diversity, combined with the relative isolation of developer communities, has resulted in a lack of comprehensive documentation and common classification, making it difficult for researchers to gain a complete understanding of the field. In this paper, we make an initial effort to establish a common taxonomy and categorize many existing Wasm runtimes. Our taxonomy classifies Wasm runtimes into five broad categories: type, architecture, platform, compilation mode, and execution environment. difficult We believe that this paper provides a valuable framework for describing WebAssembly runtimes and select- ing, examining, and comparing runtime systems based on their capabilities. This foundation allows for the classification of additional runtime systems using our definitions and offers a better overview and comparative basis for newly imple- mented features within the diverse and expanding field of WebAssembly runtime ecosystems.

References

Andreas, H., Andreas R., Derek S., Ben., T.L., Michael, H., et al. (2017). Bringing the web up to speed with WebAssembly. Pro- ceedings of the 38th ACM SIGPLAN Conference on Programming Language Design and Implementation, 185-200.

Bytcode Alliance (a). (2024). WebAssembly GC proposal. Available from: https://github.com/WebAssembly/gc.

Bytcode Alliance (b). (2024). Wasmtime - a fast and secure runtime for WebAssem- bly. Available from: https://wasmtime.dev/.

Chicory Runtime. (2024). Available from: https://github.com/ dylibso/chicory.

Extism. (2024). Extism - a lightweight framework for building with WebAssembly. Available from: https://github.com/tessi/wasmex.

Fermyon Technologies (a). (2024). Spin - a developer tool for building WebAssem- bly microservices. Available from: https://github.com/fermyon/spin.

Fermyon Technologies (b). (2024). Spin, a server-side webassemnly runtime. Avail- able from: https://github.com/fermyon/spin/discussions/ 2534discussioncomment- 9587850.

Jangda, A., Powers, B., Berger, E.D. & Guha, A. (2019). Not so fast: Analyzing the performance of {WebAssembly} vs. native code. USENIX Annual Technical Conference (USENIX ATC 19), 107–120.

Kakati, S. & Brorsson, M. (2023). WebAssembly Beyond the Web: A Review for the Edge-Cloud Continuum. 3rd International Conference on In- telligent Technologies (CONIT), 1-8.

Lunatic Inc. (2023). Lunatic - an Erlang-inspired runtime for WebAssembly. Available from: https://github.com/lunatic-solutions/lunatic/.

McConnell, J. (2017). WebAssembly support now shipping in all major browsers. Available from: https://blog.mozilla.org/blog/ 2017/11/13/ webassembly- in-browsers.

Mohak, C., Nils, K., Jophin, J., Anshul, J., Michael, G. & Shajulin, B. (2023). Exploring the Use of WebAssembly in HPC. PPoPP ’23, Association for Computing Machinery, 92–106.

Oracle. (2024). GraalWasm - an open source WebAssembly runtime. Avail- able from: https://www.graalvm.org/latest/reference-manual/wasm/.

Radovici, A., Rusu, C. & Serban, R. (2018). A Sur- vey of IoT Security Threats and Solutions. 17th RoEduNet Conference: Net- working in Education and Research (RoEduNet).

Ray, P.P. (2023). An Overview of WebAssembly for IoT: Background, Tools, State-of-the-Art, Challenges, and Future Directions. Future Internet.

Spies, B. & Mock, M. (2021). An Evaluation of WebAssembly in Non- Web Environments, XLVII Latin American Computing Conference (CLEI), 1-10.

Tetrate.io. (2024). Wazero: the zero dependency WebAssembly runtime for Go developers. Available from: https://github.com/tetratelabs/wazero.

Wasmer Inc. (2024). Wasmer, The leading Wasm Runtime supporting WASIX, WASI and Emscripten. Available from: https://github.com/wasmerio/wasmer.

WasmCloud LLC. (2024). wasmCloud - a universal WebAssembly application platform. Available from: https://github.com/ wasmCloud/wasmCloud.

Wang, Z., Wang, J., Wang, Z. & Hu, Y. (2018). Characterization and Implication of Edge WebAssembly Runtimes, IEEE 23rd Int Conf on High Performance Computing Communications; 7th Int Conf on Data Science Systems; 19th Int Conf on Smart City; 7th Int.

Wasmex. (2024). Wasmex - a fast and secure WebAssembly and WASI runtime for Elixir. Available from: https://github.com/tessi/wasmex.

WasmEdge. (2024). WasmEdge, A WebAssembly Runtime. Available from: https://wasmedge.org/.

WebAssembly Contributors. (2015). WebAssembly Launch. GitHub Issue.

WebAssembly Working Group. (2022). WebAssembly Core Speci- fication. World Wide Web Consortium (W3C). Available from: https://www.w3.org/TR/wasm-core-2 .

WebAssembly Community Group. (2021). WebAssembly System Interface. Available from: https://github.com/WebAssembly/WASI.

Wenwen, W. (2022). How Far We've Come – A Characterization Study of Standalone WebAssembly Runtimes. 2022 IEEE International Symposium on Workload Characterization (IISWC), 228-241.

Zhang, X., Liu, M., Wang, H., Ma, Y., Huang, G. & Liu, X. (2024). Research on WebAssembly Runtimes: A Survey. Available from: https://arxiv.org/abs/2404.12621.

Khazar Journal of Science and Technology `Volume 9 №1 2025, 47-59
 DOI: 10.5782/2520-6133.2025.9.1.47

Sentiment Analysis Using Machine Learning Methods on Social Media

Jamila Damirova[1], Leyla Muradkhanli[2]
[1,2] Khazar University, Baku, Azerbaijan
[2]Baku Higher Oil School, Baku, Azerbaijan
Corresponding author: jdamirova@khazar.org

Abstract
Sentiment analysis deals with understanding human feelings and opinions by analyzing the emotional content of words. With the rise of social media platforms, an immense volume of text data has become available for analysis. Machine learning (ML) techniques are essential to process this data and can provide businesses with deep insights into customer feedback, brand reputation, and emerging market trends. They also help governments and public organizations gauge public opinion on current events, proposed laws, and social issues. This study aims to improve the accuracy and effectiveness of sentiment analysis on social media (specifically Twitter) by applying advanced ML methods to address challenges of contextual understanding, noisy text preprocessing, and the evolving slang and vernacular of online content. We developed a sentiment classification model for Twitter data and evaluated several algorithms on a real-world dataset. The results show that a ML approach can successfully classify social media posts by sentiment, highlighting prevailing public moods in real time. In our experiments, an ensemble model outperformed other classifiers in balancing precision and recall, achieving high overall accuracy. These findings showcase the potential of ML methods in capturing the sentiment of social media discourse.

Keywords: sentiment analysis, social media, Twitter, machine learning, data mining.

Introduction
Sentiment analysis (also known as opinion mining) centers on extracting and identifying subjective information from text to determine the sentiment (positive, negative, or neutral) expressed by a writer or speaker. The explosion of user-generated content on social media has created a vast repository of textual data that organizations can analyze to understand public emotions and opinions. However, the sheer volume and informal nature of social media text make manual analysis infeasible, necessitating automatic methods. Machine learning has become indispensable in this context,

enabling the efficient processing and analysis of massive datasets of tweets, posts, and comments.

Social media sentiment analysis can yield valuable insights across various domains. Businesses can mine online reviews and comments to gauge customer satisfaction and brand reputation, informing their marketing and customer service strategies. Public agencies can monitor sentiment on platforms like Twitter to understand citizens' reactions to events, policies, or social issues, allowing timely and informed responses. Prior work has demonstrated that Twitter data can be leveraged for sentiment analysis to reflect collective attitudes and even predict socio-economic phenomena (Liu, et al., 2021). At the same time, analyzing social media poses unique challenges. The language used in tweets and posts is often informal and filled with slang, abbreviations, emojis, and sarcasm. For example, a phrase like "yeah right" might actually imply a negative sentiment despite positive wording, and a "😂" emoji can intensify the positive sentiment of a funny remark. Effective sentiment analysis models must handle such nuances, including negation (e.g. *"not bad"* conveying a positive sentiment), context dependence, and the presence of multimedia elements or memes that provide additional context to text. Furthermore, social media content can be extremely **noisy** – rife with spelling errors, internet slang, and inconsistent grammar – which makes preprocessing a crucial step before analysis.

In this research, we focus on applying ML methods to Twitter, a popular social media platform, to classify the sentiment of posts. The goal is to achieve high accuracy in sentiment classification by addressing the aforementioned challenges. To accomplish this, we employ modern natural language processing techniques such as word embeddings to capture contextual meaning, and we experiment with multiple classification algorithms to find the most effective model. We pay special attention to issues like class imbalance (since datasets may have more of one sentiment than another) and the dynamic language of social media. By extensively training and validating our models, we ensure they are robust against the diverse and evolving nuances found in tweets. Ultimately, improving sentiment analysis on social media not only contributes to academic research but also has practical implications – it better equips us to interpret "digitized" emotions in real time, enhancing decision-making in areas ranging from marketing to governance.

Literature review

Sentiment analysis, which can also be referred to as opinion mining, is the process of identifying and extracting subjective information from source

materials. Machine learning, natural language processing, and text analytics are applied to conduct sentiment analysis. Its purpose is to ascertain the viewpoint, feeling, or attitude of a speaker or writer with regard to some particular subject or the overall polarity of the expression.

Basically, sentiment analysis is about how feelings can be interpreted and classified in terms of sentiment in text. Several research works have been conducted to apply a wide range of ML strategies in an effort to improve precision and efficiency in sentiment analysis.

Regarding the work done in 2002, Pang et al. worked on the task of classifying movie reviews as either positive or negative. To approach this sentiment analysis task, they employed a number of ML techniques, including Naïve Bayes, Maximum Entropy classifier, and Support Vector Machines (SVM). The dataset used consisted of movie reviews from the IMDb website. The researchers conclude "that the best performance was achieved by SVMs, which outperformed all the other algorithms significantly, in particular when unigram features are used" (Pang, et al., 2002).

There were a number of limitations in this study: it was limited to just reviews of movies written in English, so the possibility of doing sentiment analysis in many languages is open to question. Second, it failed to address the problem of data imbalance, where the number of positive evaluations may considerably outweigh the number of negative reviews or vice versa. Third, the tried methods did not work very well in accommodating the tone of idiomatic phrases containing sarcasm or irony in the text. The final limitation of this research is that it did not consider deep learning algorithms, which at the time of the study were still in their infancy but today have shown promise in handling more complex linguistic structures.

This work opened several doors to possible future investigation. First is the investigation of increasingly complicated feature sets and ML models – each of which could better capture nuances of emotion. Another concern that remains unanswered is how these methods may be modified to work in another domain or language, especially when the textual data is not as straightforward as movie reviews.

In another influential study, Turney (2002) focused on unsupervised learning methods for sentiment analysis. Turney analyzed feelings expressed in product reviews using a method based on pointwise mutual information (PMI). The algorithm determined the overall sentiment of reviews by extracting significant terms from the text and comparing their PMI scores with predefined "positive" and "negative" reference words. The study concluded that an unsupervised learning approach can achieve accuracy comparable to that of supervised techniques (Turney, 2002).

Despite that success, a number of limitations remained with Turney's study. First, the approach's success depended upon the correctness and appropriateness of the chosen reference words, making it susceptible to bias or misselection of those words. The second limitation pertained to the approach's inefficiency with phrases containing sarcasm, irony, and other forms of subtle sentiment – such complexities were not effectively captured by PMI. Third, the research only considered reviews written in English; hence, the question of whether this method can be adapted for use with other languages was left open. Lastly, the researchers did not compare their unsupervised approach with alternative methods, leaving room for further comparative studies.

Future research following Turney's work could focus on improving the selection of reference terms, broadening the method's applicability to multi-lingual and multi-domain scenarios, and devising ways to capture more complex emotions such as irony and sarcasm. There is also an opportunity to compare PMI-based methods against other unsupervised techniques to determine which yields superior performance under various conditions.

Dave et al. (2003) studied the classification of online product reviews using ML methodologies. These researchers published a paper in 2003 addressing this problem. They focused on customer reviews of products and employed algorithms such as Naïve Bayes classifiers to automatically determine if feedback was positive or negative in tone. The study concluded that Naïve Bayes classifiers are efficient; hence, they could be practically used to classify customer reviews on e-commerce websites (Dave, et al., 2003).

A more recent work by Wang et al. (2021) provided *"A Survey on Session-based Recommender Systems."* Despite the title, this paper includes a literature review of ML methods in the context of social media analytics. The authors summarize various ML techniques for tasks such as sentiment analysis, event detection, and social network analysis on social media. They categorize these tasks into broad categories: content-based analysis, user and network analysis, and hybrid analysis that incorporates both content and network features. The authors discuss traditional ML algorithms like Naïve Bayes, SVM, and Random Forest, as well as emerging techniques based on deep learning. While ML has considerably advanced the field of social media analytics, the authors conclude that there is still room to develop more effective real-time models (Wang, et al., 2021).

However, the survey by Wang et al. has some limitations. It does not provide an extensive comparative analysis between the ML methods it discusses – such comparisons are largely left to the reader's interpretation. It also does not deeply explore the ethical issues associated with data mining in social media, such as privacy and bias in algorithms. Additionally, the paper

assumes some background in ML; readers lacking this background might find it challenging. Finally, although the need for real-time analytics in social media is mentioned, the survey offers no concrete solutions or suggestions to achieve it. This leads to several open questions: On what basis can one objectively compare the effectiveness and efficiency of various ML methods? What are the ethical issues related to data privacy and bias when using these methods, and how can models be made more transparent and interpretable to non-specialists? How can we provide effective real-time analytics in the fast-paced context of social media? These questions continue to motivate research in the field.

Tang et al. (2014) investigated the impact of various ML algorithms for sentiment analysis on social media, including some unsupervised feature learning techniques for user behavior analysis on social platforms. In their study, they leveraged large datasets from popular websites such as Facebook and Twitter. The broad objective was to understand which factors influence sentiment prediction when considering different elements like user engagement and content type. They experimented with a combination of supervised and unsupervised learning approaches and reported impressive sentiment classification accuracies from their models (Tang, et al., 2014).

However, Tang et al. also faced challenges. One issue was handling bilingual information on international platforms, which led to some errors since their model training was primarily on English-language data – this might fail to capture subtleties in other languages. Additionally, their work did not delve into contextual word embeddings (which have since become important for interpreting sentiment in short social media posts). The authors noted that social media language and trends change very quickly, potentially requiring frequent model updates to remain effective. Notably, their study did not explore how newer architectures like transformer-based models could be applied to sentiment analysis on social media. Social media text often includes difficult elements such as irony and sarcasm that are tricky to interpret and handle. There is also more to learn about how textual sentiment interacts with visual content (for example, the sentiment conveyed by images, GIFs, or memes accompanying text). These areas remain ripe for further research to enhance sentiment analysis in the social media domain.

Methodology

To carry out this research, we followed a structured process that includes data collection, preprocessing, feature extraction, model training, and evaluation. Below, we outline each step of the methodology and the ML algorithms applied in the research.

Data collection. A dataset of tweets from Twitter have collected to serve as the basis for sentiment analysis. In particular, the data focused on a relevant case study – tweets related to a notable aviation incident and its aftermath. Using the Twitter API, we retrieved posts that contained specific keywords and hashtags associated with the event. To ensure the data was relevant and manageable, we filtered tweets by language (keeping only those in Azerbaijani, the primary language of the discussed incident) and removed any retweets or duplicate entries. The final dataset provided a diverse sample of public opinions, including both original tweets and user replies, capturing reactions and sentiment around the incident over a defined time frame. Metadata such as timestamps and user information was collected alongside the text content to enrich the context if needed, though the sentiment analysis itself focused on the textual content of the tweets.

Data preprocessing. Raw social media data is often noisy, so preprocessing was essential to clean and prepare the tweets for analysis. We utilized the Natural Language Toolkit (NLTK) in Python to tokenize each tweet (splitting text into words or tokens) and to remove irrelevant characters. This step involved converting all text to lowercase and eliminating URLs, user mentions (e.g. @username), hashtags (while retaining the hashtagged word itself), punctuation, and other special symbols that do not contribute to sentiment. We also removed common stop words (such as “and”, “the”, “is”) that carry little sentiment value. In addition, we addressed informal language by normalizing slang and abbreviations (for example, converting “u” to “you” and “rly” to “really”) so that the words could be recognized by our models. We did not remove emoticons and emoji characters, as these can carry sentiment – instead, we translated them into textual cues (for instance, replacing “:)” with the word “smiley”). Finally, we handled negation by noting cases where words like “not” or “never” appear, since they can flip the sentiment of phrases that follow. After these cleaning steps, each tweet was left as a sequence of meaningful tokens ready for feature extraction.

Feature extraction. Rather than using simple bag-of-words representations, we employed **word embedding** techniques to capture the context and semantic meaning of words in the tweets. In particular, we utilized the Word2Vec model to transform each token (word) into a continuous vector representation. Word2Vec is an unsupervised learning approach that learns dense vector representations of words from a corpus, such that words with similar meanings end up with vectors that are close in the multi-dimensional vector space (Pak and Paroubek, 2010). We trained a Word2Vec model on a large collection of tweets (including our dataset and additional Twitter data for better coverage of the language) to obtain high-quality embeddings for Azerbaijani and mixed-language slang words. Each tweet in our dataset was

then represented as a combination of these word vectors. For simplicity and efficiency, we used the average of the word vectors in a tweet to form a single fixed-length feature vector for that tweet. This approach yields a vector representation that encapsulates the general semantic tone of the tweet while being robust to variations in tweet length. In addition to embeddings, we experimented with a few additional features: for example, we recorded the length of each tweet (number of words) and the count of strongly positive or negative words (based on an external sentiment lexicon) present in the tweet. These features were appended to the feature vector, with the aim of providing the learning algorithms some straightforward indicators of sentiment intensity (e.g., a very long tweet might indicate a detailed rant or explanation, and multiple strong sentiment words might indicate an intense sentiment). The final feature set for each tweet thus included both the learned semantic features from Word2Vec and a small number of engineered features like tweet length.

Model training. We evaluated several supervised ML algorithms to classify tweets into sentiment categories (positive or negative, given that neutral tweets were sparse in our focused incident dataset). The models we developed and tested include **Logistic Regression**, **SVM**, and **Random Forest** classifiers. These algorithms were chosen to represent a mix of simple, well-understood models and more powerful ensemble methods. Logistic Regression is a linear model that often serves as a strong baseline for binary classification due to its simplicity and effectiveness. The SVM is a robust classifier that can handle high-dimensional feature spaces and is known for maximizing the margin between classes, which is useful given the nuanced differences between positive and negative sentiment. The Random Forest is an ensemble of decision trees that aggregates the predictions of many trees, offering improvements in accuracy and robustness by reducing overfitting. We implemented all three models using the scikit-learn library in Python, which provides efficient and optimized versions of these algorithms. All models were trained on the same labeled dataset of tweets with manually assigned sentiment labels (our ground truth). We used 70% of the data for training and reserved 30% as a test set to evaluate performance on unseen data. During training, we applied techniques to address class imbalance: since negative tweets were more common in our dataset (due to the nature of the incident), we employed stratified sampling to ensure the training process saw a proportional mix of sentiment classes, and we gave the minority class a slightly higher weight in the loss function for algorithms that support weighting. We also performed hyperparameter tuning for each model using cross-validation on the training set – for example, testing different values of the regularization strength in Logistic Regression, the kernel type and C

parameter in SVM, and the number of trees in the Random Forest – selecting the settings that yielded the best average performance on validation folds.
Evaluation. After training the models, we evaluated their performance on the held-out test set. We used standard classification metrics to measure effectiveness: **accuracy** (the overall fraction of tweets correctly classified), **precision** (the accuracy of positive sentiment predictions), **recall** (the ability to capture all actual positive sentiments), and **F1-score** (the harmonic mean of precision and recall). These metrics were computed for each model to facilitate a comparison. In addition, we plotted the **confusion matrix** for each classifier to visualize how many positive tweets were correctly identified versus misclassified, and similarly for negative tweets. The confusion matrix provides insight into the types of errors the model makes – for instance, whether it tends to falsely label negative tweets as positive or vice versa. We also examined the **Receiver Operating Characteristic (ROC)** curve and computed the **Area Under the ROC Curve (AUC)** for each model, which is useful for evaluating performance on imbalanced datasets. An AUC close to 1 indicates excellent discriminative ability between classes. Finally, to interpret the Random Forest model, we extracted the feature importance scores it assigns to each input feature. This helped us understand which features (or words) had the most influence on the model's decisions. As expected, the word embedding features collectively accounted for the majority of the importance in the Random Forest's predictions, indicating that the semantic content of the tweets was the primary driver of sentiment classification. Some simple features, such as tweet length, had smaller but non-negligible importance (for example, extremely short tweets tended to be neutral or ambiguous, while very long tweets often carried strong sentiment). This interpretability step ensured that our models are not just accurate, but also somewhat explainable in terms of what factors they consider important.

Experimental results
After implementing the above methodology, we compared the performance of the three ML models on the Twitter dataset. Table 1 below summarizes the evaluation metrics for each classifier on the test set:

Table 1. Sentiment classification performance on Twitter dataset

Model	Accuracy	Precision	Recall	F1-score
Logistic Regression	0.85	0.84	0.81	0.82
SVM (RBF Kernel)	0.91	0.92	0.88	0.90
Random Forest	0.89	0.87	0.90	0.88

Among the models tested, the SVM and Random Forest classifiers delivered the best results. The SVM achieved the highest overall accuracy on the test data (around 90% correct classifications) and the highest precision, meaning it was very effective at identifying positive tweets correctly with few false positives. The Random Forest model, on the other hand, had a slightly lower accuracy than SVM but excelled in recall – it caught a higher proportion of the truly positive tweets – and maintained a strong precision as well. In terms of the harmonic mean of precision and recall (F1-score), both SVM and Random Forest were quite close. Logistic Regression, as expected for a baseline model, showed decent performance (around 85% accuracy) but trailed the other two in precision and recall. It is worth noting that all three models performed substantially better than random guessing, indicating that the features extracted (especially the word embeddings) carry significant sentiment signal. We also observed that the ML models generalized well: the training process and cross-validation ensured that we did not severely overfit to the training data. This is evidenced by the high accuracy and F1-scores on the independent test set. Figure 1 illustrates the confusion matrix for the Random Forest classifier, which provides further insight into its performance.

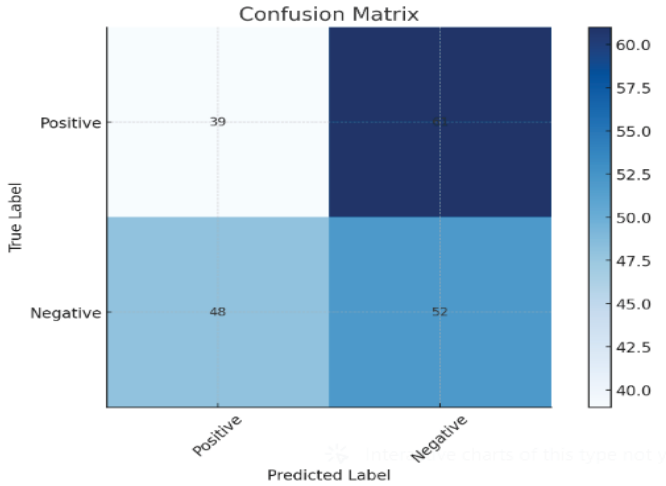

Figure 1. Confusion matrix for the random forest classifier.

The diagonal elements of the matrix (true positives and true negatives) are significantly higher than the off-diagonals, showing that the model correctly classifies most tweets in both positive and negative categories. There is a relatively small number of false positives (negative tweets misclassified as positive) and false negatives (positive tweets misclassified as negative), which aligns with the model's balanced precision and recall. We also

generated similar confusion matrices for the SVM and logistic models (not shown here for brevity), which reflected their respective strengths and weaknesses (the SVM's errors were slightly fewer overall, while the logistic regression's matrix showed more false negatives than the others).

In addition to overall performance, we analyzed which features were most influential in the Random Forest model's decisions. The feature importance scores from the Random Forest confirmed that the word embedding features were by far the most important inputs for predicting sentiment. This makes sense, as the embedding dimensions encode nuanced semantic information about the presence of positive or negative words and contexts in each tweet. In comparison, the few handcrafted features had smaller importance values. For instance, the length of the tweet contributed some predictive power (very long tweets in our dataset were often detailed explanations of the event which skewed negative in sentiment), but its importance was much lower than that of any dimension of the learned embeddings. No single word or feature dominated the predictions; rather, the model considered a combination of many embedding features to make a decision. This indicates that our model is truly learning a distributed representation of sentiment – it's not just counting smiley faces or specific keywords, but assessing the overall context of words in the tweet. This result highlights the benefit of using word embeddings and an ensemble model: the approach captures subtle signals (like tone and context) that simpler features might miss, leading to more reliable sentiment predictions.

Having selected the Random Forest as the most balanced and interpretable model, we applied it to analyze the overall sentiment trends in the collected Twitter data about the aviation incident. The majority of tweets were classified as negative in sentiment, reflecting an overall unfavorable public reaction to the incident. This aligns with expectations, as the scenario involved a plane crash and contentious circumstances that would naturally elicit public anger, fear, or frustration. Upon closer inspection of model outputs and example tweets, we found that many negatively classified tweets contained words and phrases expressing outrage at the entities perceived to be responsible (with numerous posts blaming or criticizing officials and highlighting the alleged involvement of foreign actors in the incident). For instance, a significant number of tweets blamed a certain country's air defense for the crash and demanded accountability, which the model reliably tagged as negative in tone. On the other hand, a smaller portion of the tweets were classified as positive. These were largely messages praising the heroic actions of individuals related to the incident – for example, tweets commending the airplane's pilot for a safe emergency landing or appreciating the comforting statements made by a flight attendant. Such tweets carried a

tone of admiration or gratitude. Our model successfully identified these as positive outliers against the prevailing negative background. We also observed some tweets labeled as positive that used humor or sarcasm to cope with the situation; interestingly, the model occasionally struggled with sarcastic humor when no clear positive or negative keywords were present, highlighting an area for improvement.

Overall, the experimental results demonstrate that our ML approach is effective in capturing the dominant sentiment in social media discussions. The Random Forest model provided a well-rounded performance, managing to detect the overarching negative sentiment while also picking up on positive sentiments where present. These practical findings underscore the value of automated sentiment analysis: by processing tweets at scale, we were able to quantify public emotion (e.g., "X% of tweets were negative") and extract key themes driving those sentiments, all in a relatively short time after data collection.

Figure 2 provides a visual summary of the sentiment classification, showing the proportion of tweets in each sentiment category as determined by our best model. In this case study, the negative sentiments overwhelmingly surpassed the positive ones, a result that was expected given the nature of the event. Such visualizations and quantitative results can be extremely useful for decision-makers – for example, authorities can use this information to understand public grievances, and companies can similarly gauge customer satisfaction levels on social media. Importantly, our results also highlight that even in a multilingual setting with informal language (Azerbaijani social media content with slang), classical ML methods with appropriate feature engineering can achieve high accuracy. This provides a baseline for future improvements using more complex models.

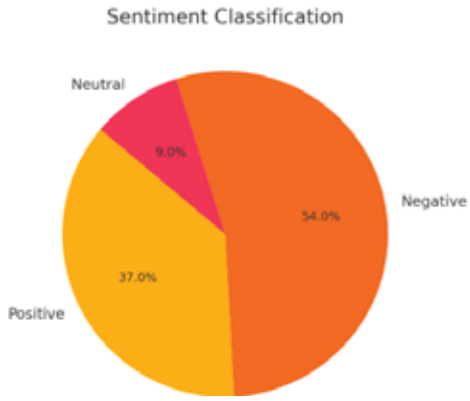

Figure 2. Sentiment classification distribution.

Conclusion

In summary, this research demonstrated that ML methods can be effectively applied to sentiment analysis on social media data, with promising results. By building a pipeline that included robust data preprocessing and modern feature extraction (word embeddings), we were able to train classifiers that accurately discern positive vs. negative sentiment in tweets. Among the algorithms evaluated, an ensemble approach (Random Forest) achieved the best balance of performance metrics, slightly outperforming a SVM in our case study. The Random Forest model's strength lies in its ability to aggregate information from multiple decision trees, which proved beneficial for capturing the varied expressions of sentiment in noisy social media text. The models not only performed well on the test data, with accuracies around 85–90%, but also provided interpretable insights through feature importance analysis. This indicates that our approach is both effective and explainable to a degree, a combination that is valuable for practical deployments of sentiment analysis systems.

The findings from the experimental analysis of tweets regarding the aviation incident revealed that public sentiment was predominantly negative, as expected. The automated sentiment analysis correlated well with the real-world context: the negative tweets reflected public frustration and calls for accountability, whereas the positive tweets highlighted commendable actions and offered support. These insights illustrate how sentiment analysis can turn unstructured social media chatter into structured information about public opinion. In real-time scenarios, such a system could help organizations and authorities quickly grasp the emotional climate following an event or announcement. For example, companies can track spikes in negative sentiment after a product launch to identify potential issues, and government agencies can monitor social media sentiment to inform their public communication strategies during a crisis.

It is also important to acknowledge the limitations of our study and the avenues they suggest for future work. First, while our models handled the informal language of Twitter reasonably well, sarcasm and irony remain challenging to detect accurately. A tweet might use positive words to convey a negative sentiment sarcastically, and our classical models (relying on word embeddings and frequency patterns) can sometimes be misled. Advanced deep learning architectures, such as transformer-based models like BERT, have shown superior ability to capture context and could further improve performance on such complex language features. Integrating or fine-tuning such state-of-the-art models on our dataset is a logical next step to enhance understanding of subtle sentiments. Second, our approach treated the problem as binary sentiment classification (positive vs. negative). In practice, neutral sentiments or a more fine-grained range of emotions (anger, joy,

sadness, etc.) could be considered for a more detailed sentiment analysis. Extending the classification scheme and gathering labeled data for those additional categories would make the analysis more comprehensive. Third, the domain specificity of our case study (an aviation incident in Azerbaijani Twitter) means the models learned patterns particular to that context. To generalize the solution, one could employ transfer learning techniques or train on a more diverse dataset so that the model can adapt to different topics and languages. Finally, ethical considerations should be kept in mind: analyzing user-generated content must respect privacy, and the deployment of sentiment analysis in decision-making should be done transparently to avoid unintended bias or misuse. Despite these considerations, our work demonstrates a successful application of ML to gauge public sentiment on social media. As social networks continue to play a central role in shaping and reflecting public opinion, the ability to automatically and accurately interpret the sentiment behind online posts is an invaluable tool. It allows businesses, researchers, and policymakers to tap into the collective mood of the public, respond to concerns, and understand the impact of events in real time. The continuing advancement of ML methods, along with careful handling of the challenges unique to social media data, will further enhance the accuracy and usefulness of sentiment analysis in the years to come.

References

Dave, K., Lawrence, S., & Pennock, D. M. (2003). Mining the peanut gallery: Opinion extraction and semantic classification of product reviews. In Proceedings of the 12th international conference on World Wide Web, 519-528.

Liu, R., Yao, X., Guo, C., & Wei, X. (2021). Can we forecast presidential election using twitter data? an integrative modelling approach. Annals of GIS, 27(1), 43-56.

Pang, B., Lee, L., & Vaithyanathan, S. (2002). Thumbs up? Sentiment Classification using Machine Learning Techniques. In Proceedings of the ACL-02 conference on Empirical methods in natural language processing-Volume, 10, 79-86.

Pak, A., & Paroubek, P. (2010). Twitter as a Corpus for Sentiment Analysis and Opinion Mining. In Proceedings of the International Conference on Language Resources and Evaluation (LREC), pp. 1320–1326.

Tang, J., Chang, Y., & Liu, H. (2014). Mining social media with social theories: a survey. ACM Sigkdd Explorations Newsletter, 15(2), 20-29.

Turney, P. D. (2002). Thumbs Up or Thumbs Down? Semantic Orientation Applied to Unsupervised Classification of Reviews. Proceedings of the 40th Annual Meeting on Association for Computational Linguistics, 417-424.

Wang, S., Wang, Y., Sheng, Q.Z. & Orgun, M.A. (2021). A survey on session-based recommender systems. ACM Computing Surveys (CSUR). 54(7), 1-38.

Khazar Journal of Science and Technology `Volume 9 №1 2025, 60-65

DOI: 10.5782/2520-6133.2025.9.1.60

Research of Purification of Oil Sludge Waste Mixture Using $Fe_2(SO_4)_3$ As A Coagulant

Tahmina Osmanova, Sevinj Hajiyeva, Qiyas Bayramov
Ecological Chemistry Departament, Baku State University, Baku, Azerbaijan
Corresponding author: t.a-1990@mail.ru

Abstract
During the treatment of industrial waste water (IWW) formed in technological processes at the Heydar Aliyev refinery at the plant's treatment facilities, a deposition of oil sludge waste mixture (OSWM) with various composition and properties takes place on the bottom of these facilities. The definition of composition and properties of OSWM is not the main purpose of this research work. But according to the information given in the technical literature, it can be noted that OSWM contains ~5-90% oil (or oil products), 1-52% water, 0.8-65% solid impurities, the density of oil sludge is 1.5-2 g/cm^3, pour point from -3°C to +80°C, flash point from 35°C to 120°C. Not only in our country, but throughout the world the problem of deep (up to 100%) ecologically effective purification of this mixture from the oil products waste mixture (OPWM) has not been completely solved until now. Despite the use of various coagulants ($AlCl_3$, $FeCl_3$, polyacrylamides, polyaluminum silicate chloride, polyferric silicate chloride), the maximum efficiency of purification of OSWM from OPWM was ~95% when carrying out the purification process in several stages. We conducted a study of purification of this mixture samples taken from the input of "Alpha-Laval" facility, processing OSWM at the above-mentioned plant (from the area where OSWM was collected for processing) using $Fe_2(SO_4)_3$ as a coagulant. The choice of this coagulant is explained by the fact that the purification process of OSWM is simple, economically beneficial, meets all environmental safety requirements, and is carried out at room temperature. Based on the results of the study, it was established that the highly effective purification of the OSWM sample using a solution of $Fe_2(SO_4)_3$ as a coagulant initially depends on the choice of an extractant, the volume of a coagulant, mixing time, the development of special optimal conditions. Treatment of OPWM from the OSWM up to 96.87% was achieved. Optimal conditions specially developed for this consist of using 5 ml of a primary gasoline fraction which is cheaper than petroleum ether as an extractant, 25 ml of a 5% solution of $Fe_2(SO_4)_3$ as a coagulant, 10 ml of H_2SO_4 as a flocculant and interval mixing of the mixture during 6 hours at room temperature..
Keywords: Oil sludge, coagulant, extractant, production, waste water, petroleum ether, gasoline fraction, optimal conditions.

Introduction

As noted in the scientific and technical literature, the 100% separation of the oil or OPWM contained in the oil sludge waste formed in the oil production and refining industry has not been achieved so far. It can be noted that the OSWM formed in the oil refining industry is very complex due to the composition and nature in comparison with the oil sludge waste of the oil production industry. That is why, together with IWW, which is formed during various technological processes in the oil refining industry, oil sludges with various composition enters the treatment facilities of the enterprise. The methods used in production and also developed in the research works on the separation of OPWM from the OSWM accumulated at the bottom of these treatment facilities by many researchers earlier for the stated purpose are not 100% effective.

As mentioned in the literature (Bagryantsev, et al., 1995; Vaisman, 2010), the deep and ecologically effective cleaning of OSWM with modern methods has not yet been fully achieved, because each of them has ecological and economic shortcomings.

At present, in general in the oil industry, a large amount of energy and financial costs are spent during the operation of each facility that carries out the processing of the OSWM (the separation of oil or OPWM from its composition).

Taking into account the brief explanations given above, we carried out research works on the ecologically effective purification of the OSWM from the OPWM in several directions in order to determine the purification effectiveness of coagulant substances. One of these research works was carried out using $Fe_2(SO_4)_3$ in accordance with the research works developed by us and noted in the literature (Bayramov, et al., 2018; Osmanova, 2022), the study on the purification of the OSWM sample was carried out in the following way.

Experimental Parts

In accordance with the research works presented in the literature (Bayramov, et al., 2018; Osmanova, 2022), we report the progress of determining the effectiveness of treatment of the mentioned sludge waste with complex composition with this substance by using the initial gasoline fraction as an extractant and a 5% solution of $Fe_2(SO_4)_3$ salt as a coagulant for chemical treatment of the OSWM sample in the laboratory conditions.

Based on the results of the research conducted by us, 50 g of the OSWM is placed in the reaction flask and 200 g of unrefined IWW from the plant is added to it and mixed during 1 hour. Then the mixture is filled into the separating funnel and mixed. 5 ml of the initial gasoline fraction is added to

the mixture and mixed at the room temperature with breaks during 2 hours. In each experiment, 5% solution of $Fe_2(SO_4)_3$ is added to the mixture in the quantities indicated in the table 1 and mixed with breaks during 4 hours.
After the process of obtaining three phases (solid, water and organic layers) in the separating funnel is completed, each of these layers is filled into small-volume glass flasks, the weight of which is determined in advance, and then the quantity of these layers is determined. The degree of purification of oil sludge waste from the OPWM by the method mentioned above was calculated using the indicators of the specified quantities of the OPWM, water and mechanical mixture contained in the OSWM sample used during treatment.

Result

The results of the research on purification of the OSWM from the OPWM using 5% solution of $Fe_2(SO_4)_3$ are presented in the table 1.

Table 1. The results of the research on purification of the OSWM from the OPWM using 5% solution of $Fe_2(SO_4)_3$

The OSWM sample								effectiveness of the purification with other coagulants, %	
quantity, g., purification temperature	composition before purification			reagents used for the purification		composition after purification		effectiveness of purification with $Fe_2(SO_4)_3$, %	$FeSO_4$	$FeCl_3$
	quantity of the OPWM%	quantity of water %	quantity of the mechanical mixture%	volume of an extractant, ml	volume of a 5% solution of $Fe_2(SO_4)_3$, ml	quantity of the OPWM, %	purification time, hour			
50,	60,15	24,01	15, 84	5,0	5,0	66,46	6	33,5	19,6	34,63
					10,0	48,95	6	51	37,19	51,46
					15,0	09,24	6	90,8	61,33	81,39
					20,0	05,73	6	94,3	89,82	84,98
					25,0	03,18	6	96,8	70,31	88,58
					30,0	16,57	6	83,4	36,91	48,86
					35,0	29,16	6	70,8	13,13	37,49
					40,0	28,54	6	61,5	3,38	27,74

As can be seen from the Table 1, the effectiveness of purification of the OSWM sample from the OPWM decreases if, after addition of the extractant

to the mixture, the volume of 5% solution of $Fe_2(SO_4)_3$ is more than 25 ml. Thus, the above-mentioned optimal conditions and 96.82% effectiveness of purification of the OSWM from the OPWM can be achieved by using mainly 5% solution of $Fe_2(SO_4)_3$ as a coagulant.
The graph of the dependence of the coagulation process effectiveness during the purification of the OSWM from the OPWM on the concentration of the coagulant is shown in Figure 1.

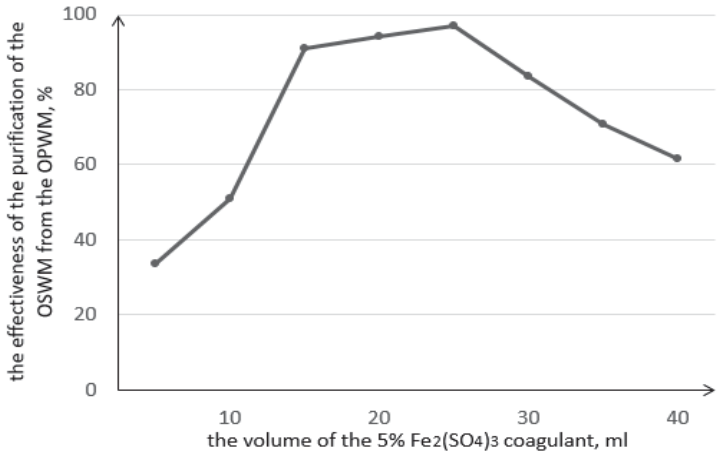

Figure 1. The graph of the dependence of the coagulation process (effectiveness of the purification of the OPWM) on the volume of 5% $Fe_2(SO_4)_3$ coagulant

The presented research work is one of the research works carried out in order to determine the effectiveness of coagulants used for chemical (coagulation) purification of the OSWM samples formed at the Heydar Aliyev refinery and taken from the field of processing at the "Alpha-Laval" facility.
There is $Fe(OH)_3$ together with sulfate salts in the IWW obtained during the process of purification of the OPWM from the OSWM using the initial gasoline fraction as an extractant, a 5% solution of $Fe_2(SO_4)_3$ salt as a coagulant, and the separated OPWM contains an extractant. Therefore, during the next purification of the OSWM the possibility of using of the IWW containing $Fe(OH)_3$ instead of a coagulant up to 15% of the slurry mixture has been determined. At the same time, in the next process of purification of the OSWM research work was carried out on the possibility of using of the OPWM containing gasoline fraction instead of an extractant up to 5% of the purified slurry mixture. The obtained results were consistent with the results of the previous research work.

Scientific explanations about the reason for the occurrence of the coagulation process are widely interpreted in the literature (Bayramov, et al., 2018; Bayramov, et al., 2019; Osmano, 2020, Osmanov, 2022). Based on these explanations, it can be noted that when a 5% solution of $Fe_2(SO_4)_3$ salt is used as a coagulant, this substance is hydrolyzed in the aquatic environment in a short period of time and $Fe(OH)_3$ is obtained.

$Fe_2(SO_4)_3 + 6H_2O \leftrightarrow 2Fe(OH)_3 + 3H_2SO_4$

$SO4^{-2}$ anions react with carbonates in the environment and various sulfate salts are obtained. The compound $Fe(OH)_3$, formed in a short period of time, collapses at the bottom part due to the attracting solid particles to itself like $Al(OH)_3$ and increasing of gravity force. When the concentration of $Fe_2(SO_4)_3$ coagulant is too high, the amount of $Fe(OH)_3$ multiplies. Therefore, $Fe(OH)_3$ precipitates attracting the sludge particles containing OPWM, to itself. In this case, regardless of the amount of the extractant, the speed of coagulation process decreases and the separation of the OSWM from the OPWM also decreases.

Based on the results of the research, it can be noted that in the oil refining industry using of a 5% solution of $Fe_2(SO_4)_3$ salt as a coagulant in the way mentioned above is more preferable according to the financial and environmental indicators than the facilities that carry out the processes of separation of OSWM from OPWM, refining and are currently in operation.

That is why, in accordance with the research work carried out by us, it can be considered scientifically based that the purification of the OSWM formed in the oil refining industry from OPWM using $Fe_2(SO_4)_3$ has great economic and environmental importance.

References

Bagryantsev, G.I., et.al. (1995). Municipal and industrial waste: methods of neutralization and recycling - analytical reviews, Novosibirsk, 128-137.

Bakhonina, E.I. (1995). Bashkir Chemical Journal, vol. 22, № 1, 20-29.

Bobovich, B.B. (1999). Textbook for universities, Moscow, 445.

Chalov, K.V. (2013). Abstract of the dissertation of a candidate of technical sciences, Moscow, 18.

Davydova, S.L. et.al. (2004). Study guide, Moscow, 163.

Grinin, A.S. et.al. (2002). Study guide, Moscow, 336.

Kablov, V.F., et.al. (2004). Research report of the Volzhsky Polytechnic Institute, 2.

Lotosh, V.E. (2007). Recycling of environmental waste, Ekaterinburg, 503

Mazlova, E.A., et.al. (2001). Study guide, Moscow, 52.

Potashnikov, Y.M. (2004). Study guide, Tver, 107.

Vaisman, Y.I. (2010). Scientific research and innovation, vol. 4, № 3, 21-27

Bayramov, Q.I., et.al. (2018). Collection of scientific papers based on the results of the V international scientific and practical conference "Current issues of natural and mathematical sciences in modern conditions of the country's development", Saint Petersburg, 28-30.

Bayramov, Q.I., et.al. (2019). Proceedings of the LIII International Scientific Conference “Theoretical and Practical Issues of Modern Science”, Moscow, vol. 2, 124.

Osmanova, T.M. (2020). Natural and technical sciences, Moscow, № 3, 20-22.

Osmanova, T.M. (2022). Natural and technical sciences, Moscow, № 4, 36-40.

Khazar Journal of Science and Technology `Volume 9 №1 2025, 66-71
 DOI: 10.5782/2520-6133.2025.9.1.66

Study of Ecotoxicants in Environmental Objects Contaminated by Mining Industry Wastewater

[1]Aiten Samadova, [1]Sevinj Hajiyeva, [2]Islam Mustafayev
[1]Ecological Chemistry Departament, Baku State University, Baku, Azerbaijan
[2] Institute of Radiation Problems, Baku, Azerbaijan
Corresponding author: aytan.samad@gmail.com

Abstract
A research study was conducted on Okchuchay, which was polluted with ecotoxic compounds. In order to investigate their pollution with pollutants, the upper, middle and lower reaches of the river were compared. Their decrease is observed from upstream to downstream. But there has been an increase over time and this is related with water streams and other factors.

Keywords: Ecotoxicant, pollutant, wastewater, ecology, physicochemical parameters.

Introduction

Recently, the pollution of the environment with ecotoxic compounds remains quite relevant. Thus, the atmosphere, the lithosphere, and the hydrosphere become saturated with pollutants in environmental objects. This affects the environmental balance and creates an imbalance. From this point of view, it is very important and urgent to investigate the hydrosphere, which is the rapid migration of ecotoxicants. For this purpose, we took Okchuchay as a research object to investigate the pollution of the hydrosphere with ecotoxic compounds (https://azertag.az/xeber/Oxchuchayin_chirklenme_gostericileri_arasdirilib-2412557). The migration of ecotoxicants was observed on it, and the dynamics of their density change was determined (Shachneva, 2012; Mur, et al. 1987).

Experımental Parts

Previously, water samples were taken from parts of the area of Jahangirbeyli, Shayifli, and Burunlu. Examples taken for the study have been studied by ISO, the physical and chemical parameters of their ingredients based on DUST standards (Table 1).

We used a pH-meter for the hydrogen indicator, an oximeter for dissolved oxygen, a conductometer for electrical conductivity, an autotitrator for sodium and chloride ions, a spectrometer for sulfate, ammonium, nitrate and nitrite ions, and an optical emission and atomic absorption spectrometer for metals (Hajiyeva, et al., 2019; Lurye, 1979; Korostilev, 1981; Charikov, 1984).

Table 1. Standards of indicators determined in water

№	Name of analysis	Method
1	Hydrogen indicator	İSO 10523
2	Electrical conductivity	İSO 7888
3	Dissolved oxygen	İSO 5814
4	Sodium	İSO 6059
5	Sulfate ions	DÜST 4389-72
6	Chloride ions	İSO 9297
7	Ammonium ions	DÜST 4192-82
8	Nitrite ions	İSO 6777
9	Nitrate ions	İSO 7890
10	Metals	İSO 11885

Result

The physical and chemical parameters of the previously taken water samples were studied. Sample analyzes were conducted earlier in January for the study of ecotoxic compounds. The results for all three areas taken are given in table 2.

It should also be noted that the Maximum Permissable Concentration for Surface water (MPC) was issued on 04 January 1994 by the Inspection Committee for Ecology and Nature of the Republic of Azerbaijan with the decree of "Prevention laws of surface water from polluted water".

As can be seen from Table 2, in the section passing through Jahangirbeyli and Sayifli villages of Okchuchay, sodium is 2.3 times, in the section passing through Burunlu village 2.4 times, iron - 1.3 times in the section passing through Sayifli village, 2.2 times in the section passing through Burunlu village, molybdenum - 1.2 times in the section passing through Burunlu village, manganese – 1.4 times in the section passing through Sayifli village and 4.9 times higher than MPC in the section passing through Burunlu village.

The fact that having metals more than the normal level in the environment has a serious effect on the aquatic biota. Perhaps, when the molybdenum is too much, the aquatic organisms absorb the metal, the process of the cumulative environment begins, and then the residual organism

disappears. Manganese is one of the most dangerous pollutants of the environment. When muttagen and allergenic manganese associations are introduced into living organisms, they deplete nektons (Hajiyeva, et al., 2021; Medvedev, et al., 2017; Davidova, 1991; Hajiyeva, et al. 2018; Hajiyeva, et al., 2019).

Repeated samples were taken from the same area on 25-26.01.2023 and re-examined on them. The obtained results are shown in table 3.

Table 2. Results of physico-chemical analyses conducted on water samples taken from the territory of East Zangezur and Karabakh economic region on 16-18.01.2023

№	Name of component	Unit of measure-ment	Amount of components			Permissible viscosity limits
			Okchuchay-Zangilan district			
			Jahangirbeyli village	Sayifli village	Burunlu village	
1	Hydrogen indicator, pH	—	7.9	7.5	7.6	6.5-8.5
2	Dissolved oxygen	mqO_2/l %	8.0 83.0	7.7 81.0	7.7 80.0	≥4.0
3	Electrical conductivity	$x10^{-3}$ Sm/sm	1.793	1.873	1.886	—
4	Sodium	mq-ekv/l	16.0	16.4	16.9	7.0
5	Chloride ions, Cl^-	mq/l	18.1	17.4	18.1	350
6	Sulfate ions, SO_4^{2-}	mq/l	369.8	372.1	385.0	500
7	Ammonium ions, NH_4^+	mq/l	0	0	0.1	0.5
8	Nitrite ions, NO_2^-	mq/l	0.21	0.34	0.37	3.3
9	Nitrate ions, NO_3^-	mq/l	5.9	5.3	7.1	45.0
10	Zinc, Zn	mkq/l	14.6	20.9	145	1000
11	Iron, Fe	mkq/l	181	392	645	300
12	Cobalt, Co	mkq/l	2.83	4.4	3.41	100
13	Lead, Pb	mkq/l	1.65	1.88	3.4	30
14	Nickel, Ni	mkq/l	1.06	0.642	1.49	100
15	Molybdenum, Mo	mkq/l	108	164	302	250
16	Manganese, Mn	mkq/l	89	144	491	100
17	Copper, Cu	mkq/l	18.1	21.0	52.1	1000

As can be seen from the analysis of the analyzes (table 3), during the analysis of water samples, it was found that in the section passing through the village of Jahangirbeyli of Okhuchay, sodium was 2.3 times, in the section passing through the villages of Sayifli and Burunlu, 2.4 times, sulfate ions - 1.1 times in the section passing through the village of Jahangirbeyli, 1.2 times in the section passing through the village of Sayifli. times, 1.3 times in the section passing through the village of section passing through the village of Sayifli, 1.3 times in the section passing through the village of Burunlu, manganese - 4 times in the section passing through the village of Jahangirbeyli, 5.7 times in the section passing through the village of Sayifli, 5.8 times in the section passing through the village of Burunlu.

Table 3. Results of physical and chemical analyzes conducted on water samples taken from the territory of East Zangezur and Karabakh economic region on 25-26.01.2023

№	Name of components	Unit of measure ment	Amount of components			Permissible viscosity limits
			Oxçuçay-Zəngilan rayonu			
			Jahangi rbeyli	Sayifli	Burunlu	
1	Hydrogen indicator, pH	—	7.9	7.5	7.5	6.5-8.5
2	Dissolved oxygen	mqO_2/L %	8.7 90.0	8.9 93.0	9.0 94.0	≥4.0
3	Electrical conductivity	x10^{-3} Sm/sm	1.812	1.807	1.823	—
4	Sodium	mq-ekv/l	16.1	16.5	16.3	7.0
5	Chloride ions, Cl^-	mq/l	18.0	17.9	17.2	350
6	Sulfate ions, SO_4^{2-}	mq/l	562.0	586.3	629.3	500
7	Ammonium ions, NH_4^+	mq/l	1.2	1.33	1.6	0.5
8	Nitrite ions, NO_2^-	mq/l	0.18	0.48	0.49	3.3
9	Nitrate ions, NO_3^-	mq/l	6.22	5.63	5.46	45.0
10	Zinc, Zn	mkq/l	68.0	152	143	1000
11	Iron, Fe	mkq/l	597	908	928	300
12	Cobalt, Co	mkq/l	3.60	5.44	4.2	100
13	Lead, Pb	mkq/l	<LOD	<LOD	<LOD	30
14	Nickel, Ni	mkq/l	1.04	3.68	3.49	100
15	Molybdenum, Mo	mkq/l	223	308	327	250
16	Manqanese, Mn	mkq/l	398	574	576	100
17	Copper, Cu	mkq/l	50.5	50.4	53.2	1000

Burunlu, ammonium ions - 2.4 times in the section passing through the village of Jahangirbeyli, 2.7 times in the section passing through the village

of Sayifli, 3.2 times in the section passing through the village of Burunlu, iron - 2 times in the section passing through the village of Jahangirbeyli, 3 times in the section passing through the village of Sayifli, Burunlu 3.1 times in the section passing through the village of molybdenum, 1.2 times in the
It is clear when comparing tables 2 and 3 that there has been an increase in a short period of time. Here, when comparing MPC, it can be seen that the maximum permissible concentration in the section passing through the villages of Jahangirbeyli and Sayifli has increased by 0.01 units, and by 0.1 units in the section passing through the village of Burunlu. Although iron was not detected in the section passing through the Jahangirbeyli village, it later exceeded the maximum permissible concentration by 2 times. In the section passing through Sayifli village, the MPC increased by 1.7 units and 0.9 units. Manganese pollution exceeded the normal level by 4 times in the section passing through the village of Jahangirbeyli, in the section passing through Shayifli villages, there was an increase of 4.3 units, and in Burunlu, there was an increase of 0.9 units. Molybdenum in the section passing through the villages of Sayifli, although it was within the MPC before, an increase of 1.2 units was observed. In the section passing through Burunlu village, there is an increase of 0.1 units of MPC. The increase of sulfate and ammonium ions, which did not exceed the maximum permissable concentration before, occurred at all three points. The decrease of some parameters from upstream to downstream is related to the self-regulation-cleaning function of the river at in a specific time period.

This work was carried out with the financial support of the Azerbaijan Science Foundation-Grant №AEF-MQM-QA-1-2021-4(41)-8/07/4-M-07.

References

Charikov, A.K. (1984). Mathematical processing of chemical analysis results. L.:Chemistry. 168.

Davidova S.L. (1991). About the toxicity of metal ions. Series "Chemistry" №3, 243.

Hajiyeva, S.R., et al. (2019). Practicum of ecologycal monitoring., 140.

Hajiyeva, S.R., et al. (2021). Chemical ecotoxicology, 288.

Hajiyeva, S.R., et al. (2018). Eecological chemistry, 43-48 .

Hajiyeva, S.R., et al. (2019). Fundamentals of ecotoxicology. 123-136.

Korostilev P.P. (1981). Preparation of solutions for chemical analytical work. -M.: Nauka. 202.

Lurye U.U. (1979). Handbook of Analytical Chemistry. M.: Chemistry. 480c.

Medvedev, I.F., et al. (2017). Heavy metals in ecosystems, Saratov: «Раkурс», 178

Mur, C.B., et al. (1987). Heavy metals in natural waters.M.: Mir, 297.

Shachneva, E.U. (2012). Impact of heavy toxic metals on the environment, Scientific potential of regions for the service of modernization. № 2 (3). 127-134.

https://azertag.az/xeber/Oxchuchayin_chirklenme_gostericileri_arasdirilib-2412557-11

Khazar Journal of Science and Technology `Volume 9 №1 2025, 72-84
 DOI: 10.5782/2520-6133.2025.9.1.72

Fabrication and Tuning of the Morphological Characterization of Pvdf Based Electrospun Nanofibrous Material

Dilara Huseynova[1,2], Rasoul Moradi[2,3], Rasim Jabbarli[4]

[1] PhD student at Khazar University, Baku, Azerbaijan
[2] Nanotechnology Laboratory. Department of Chemical Engineering, School of Science and Engineering, Khazar University, Baku Azerbaijan
[3] Department of Chemical and Biological Engineering, College of Engineering, Korea University, Seoul, Korea
[4] Azerbaijan Institute of Physics Ministry of Science and Education of Azerbaijan.
Corresponding author: dilara.sadigova3377@gmail.com

Abstract

Surface protection has undergone a radical transformation thanks to nanocoatings, which provide novel approaches with enhanced durability, performance, and resistance. Because of their unique properties and wide range of applications, these coatings based on nanotechnology have attracted a lot of attention in recent years. In this work, the use of PVDF to produce electrospin fiber-oriented film coating material was examined. The technique employed to produce the aligned nanofibers is electrospinning. To investigate the alignment of the nanofiber material, we employed a directed electrical field in electrospinning apparatus. We employed atomic force microscopy (AFM) as our test. The impacts of the different types of collectors on the form of the fiber led to an increase in the alignment structure of nanofiber molecules. The results show that the morphological structure of the ordered organized nano-fibrous material that was generated is aligned.

Keywords: fibrous nanomaterial; PVDF; high electroactive phase; electrospinning; alignment; nanofiber; rotating drum.

Introduction

In the 1970s, PVDF, a polycrystalline polymer, began to attract scientific attention due to its remarkable piezoelectric qualities. A common piezoelectric semi-crystalline polymer, PVDF contains five distinct crystalline phases: α, β, δ, γ, and ε (Jayakumar *et al*., 2003). From the perspective of technical application, the α, β, and γ-phases are the most significant and prevalent among them. Due to its non-polar nature, the semi-helical alternative trans-gauche (TGTG') conformation of the α-phase, although being the most prevalent and thermodynamically advantageous

polymorph, is negligible in electronic applications. The β, γ, and δ-phases, on the other hand, are polar and hence electroactive because of the parallel alignment of their dipoles. The development of highly scalable polymer-based nanogenerators with high power density places a premium on the pseudohexagonal β-phase with all-trans (TTTT) conformation, which has exceptional piezo-, pyro-, and ferroelectric characteristics and strong spontaneous polarization. Improving the percentage of β counterpart is the primary issue when managing multi-phase PVDF for such applications. This can be accomplished in three main ways: (a) mechanically, by applying stress or tension through stretching, bending, twisting, or pressing (Prabhakaran and Hemalatha, 2013); (b) chemically, by adding appropriate filler materials (Huang, 2012) that can improve PVDF's mechanical, electrical, thermal, or optical properties through the right ion-dipole or dipole-dipole interactions. In addition to being economical, the third approach involves the creation of sophisticated multifunctional nanomaterials, which is significant from the standpoint of materials researchers (Bhattacharjee, *et al*., 2020; 4. Chen, *et al*., 2021). There is an obvious relationship between its crystal phases and its piezoelectric characteristics (Samadi, *et al.*, 2018). The most prevalent crystalline forms of PVDF are nonpolar α and polar β phases, with the β phase giving it its piezoelectric characteristics. In the past 10 years, enhancing the β phase while decreasing the α phase content in PVDF has been a prominent topic of attention. The β phase was increased by cold-drawing (stretching) (Martins, *et al*., 2014), high-pressure quenching (Tasaka and Miyata, 1985), and poling (applying a strong electric field) of PVDF (Ting, et al., 2013; Chowdhury, *et al*., 2021; Chowdhury, *et al*., 2020). By converting the α phase into the β phase under a strong electric field, electrospinning is an additional optional, straightforward, one-step technique for creating PVDF nanofibers. The β phase of the fibers is enhanced by the high voltage that is involved in this process (Mansouri, *et al*., 2019). Additionally, compared to solvent-cast films, electrospun fiber mats are far more mechanically robust and flexible (Ghosal, et al., 2018). Aligning PVDF mats enhances their mechanical, electrical, and electroactive properties, which boosts their efficacy and versatility in a variety of technological applications, especially in fields like energy harvesting, sensors, actuators, and coating materials. In the β phase of the PVDF molecule, alignment structure is observed.

An efficient method for continually and directly creating nanofibers is electrospinning. Nearly all polymer solutions, melts, emulsions, and suspensions with enough viscosity may be produced with polymer nanofibers using the electrospinning method, which is rather easy to use and convenient. Additionally, by incorporating trace quantities of polymers into the inorganic

precursors—which are typically thought of as nonspinnable—inorganic nanofibers may also be produced using electrospinning. By altering the spinning settings, the electrospun nanofibers' diameter may be adjusted from tens of nanometers to submicrons. The electrospun fiber-stacked nonwoven fabric has a porosity of about 80% and is a porous material with interconnecting submicron pores. The electrospinning fluid's unstable rheological characteristics, however, make it challenging to produce stable and continuous nanofibers with an average diameter of less than 100 nm. As a result, the electrospun nanofibrous membranes' separation applications are restricted to microfiltration, air filtration, or membrane substrate use. The development of electrospun nanofibrous composite (ENC) membranes was thus necessary to optimize the selectivity, permeability, and other separation capabilities of electrospun nanofibrous membranes in order to properly utilize them in other separation applications. The benefits of single-layered or single-component membranes are all present in composite membranes, but they offer greater versatility in terms of functional component selection (Meng, et al., 2023).

Handling an Electrospinning Procedure. The manufacturing factors, such as the applied voltage, the flow of liquid rate, and the distance between the spinneret tip and the collector, have a major impact on the synthesis of electrospun fibers and the controlling of their diameters. A high-voltage power source, a syringe pump, a spinneret (often a blunt-tipped hypodermic needle), and a conductive collector are the main parts. There are two types of power supplies: alternating current (AC) and direct current (DC). During electrospinning, surface tension leads the liquid to be extruded from the spinneret, creating a pendant droplet. The electric field is typically produced by applying a static DC high voltage to the spinneret (Xue, et al., 2019).

PVDF poling. The voltage's polarity, which can be either positive or negative, influences the kind of charges that build up on the jet's surface as well as the distribution of charged molecules inside the liquid. Certain materials, particularly electrolytes, have electrospinning capabilities that rely on the applied voltage's polarity (Terada, et al., 2012; Tong and Wang, 2012). In addition to the strength of the interactions between the jet and the external electric field, the applied voltage also directly affects the quantity of charges carried by the jet and the strength of electrostatic repulsion between the charges. Higher voltages often encourage the production of thinner fibers (Hu, et al., 2011), but they can also cause more fluid to be ejected, which results in fibers with larger diameters (Demir, et al., 2002). Electrospun fibers have also been electrospun using AC, however the jet behaves quite differently than in the DC case. Controlling the collecting mandrel's velocity in relation to the electrospinning suspension source has been used to address

fiber alignment (Ayres, et al., 2006; Nitti, et al., 2018; Mishra, et al., 2023; Sun, et al., 2010; Kim, et al., 2016; Martins, et al., 2014). Random fibers, one direction-oriented fibers, and circumferentially oriented fibers have all been produced using three different types of collectors: (1) static plate collector, (2) drum rotating collector, and (3) disk rotating collector (Ayres, et al., 2006). Electrospun chitosan nanofiber mats with random orientation could be produced using a static plate, but nanofiber mats that were aligned circumferentially and parallel to one another could be produced using a spinning disk and a rotating drum, respectively (Nitti, et al., 2018). For this investigation, the influence of this orientation has been examined and contrasted with fibers deposited utilizing various collector typologies. This technique involves aligning PVDF material using electrospinning equipment and employing atomic force microscopy (AFM) to analyze the structure and shape of the material.

The beta phase of polyvinylidene fluoride (PVDF) has unique properties that often make it desirable to enhance it. Numerous techniques have been devised to enhance the β-crystal concentration in PVDF (Mishra, *et al*., 2023). Converting α-crystal to β-crystal using solid-state drawing and/or strong electric field poling is an appealing method that can achieve a 50–85% increase in β-crystal content (Mishra, et al., 2023; Sun, et al., 2010; Kim, et al., 2016). Due to its strong ferroelectric, pyroelectric, and piezoelectric characteristics, the β-phase of PVDF is distinguished by the biggest spontaneous polarization and particular chain conformation per crystal unit cell. The highly electroactive β-phase in PVDF may be revealed by a number of techniques, including phase transition, solvent casting, nucleating fillers, electrospinning, and copolymerization of PVDF (Martins, et al., 2014; Harstad, et al., 2017; Ruan, et al., 2018; Ahn, et al., 2006; Lannutti, et al., 2007; Hunley and Long, 2008). With all of the dipolar moments oriented in the same direction, the β-phase is formed by electrospinning, which has emerged as a promising technique (Ahn, et al., 2006; Lannutti, et al., 2007; Hunley and Long, 2008). The nanofibers may be stretched mechanically to provide elongation forces during electrospinning and to arrange the lamellae into fibers that are aligned along the fiber axis (Zhou and Wu, 2015).

To improve alignment molecular structure, we queried PVDF in our experiment. Electric field stretching was employed for the aforementioned reasons in place of mechanical stretching force.

Materials and Methods. Polyvinylidene fluoride (PVDF) pellet has Mw = 1.8 × 104 with linear chemical structure $(-CH_2CF_2-)_n$ were purchased from Sigma-Aldrich,. Acetone and N, N-dimethylformamide (DMF) were purchased from Sigma-Aldrich Fe_3O_4 was obtained from Sigma-Aldrich

with an average particle size of 20-30 nm Polysorbate Tween purchased from Sigma-Aldrich and metal bar.

PVDF solution preparation. PVDF powders were dissolved using a magnetic stirrer in a 250 ml beaker at 35 rpm for two hours at a maximum temperature of 35°C. The mixture of organic solvents, DMF/acetone = 1/1 at 10 wt% (w/w), was stirred. Once the PVDF solution had completely dissolved, it was ultrasonically cleaned for two hours using the Ultrasonic Cleaner Digital Pro until it was homogeneous and bubble-free (figure 1). A solution of Fe_3O_4 nanoparticles with a 1wt% concentration was prepared by dissolving Fe_3O_4 nanoparticle powders in 50ml of DMF and adding 10ml of Polysorbate Tween as a surfactant at 30˚C while stirring at 35 rpm for two hours. After two hours, sonication was performed to get a non-homogenous solution. Following ultrasonication, a two-phase solution was created, with the electrospinning process using the upper phase.

Preparation of aligned PVDF Fiber Mats. In this investigation, mechanical stretching forces were employed in the form of electric field stretching. To achieve the aforementioned goals, a metal bar was electrospun into the PVDF nanofiber preparation process (figure 2). A metal bar was added to the grinding line of machinery. In this method, highly aligned PVDF-Fe_3O_4 nanofiber material is obtained and the β-phase content is increased as needed. Using a flow rate of 15 milliliters per hour, an output voltage of 16 kV, and a rotating drum speed of 556 rpm, PVDF-Fe_3O_4 nanofiber was created. 4 cm separated the metal bar from the revolving collector. In order to create the PVDF-Fe_3O_4 composite material, the rotating drum speed was increased while the electrical field stretching flow rate (Fe_3O_4) = 0.5 ml/hr was the only source of force. To feed the polymer and Fe_3O_4 solution, a dual channel programmable syringe pump was developed. Both the drum spinning collector and the static plate collector have been employed independently (figure 3).

Morphological structure analysis. Atomic force microscopy (AFM) and optical microscopy are used to analyze morphological aspects. AFM is a novel technology that uses a thin tip to scan a material in order to gain images and map the surface's contours, usually at the atomic level. Three-dimensional topography and plainly identifiable morphological structure are features of AFM pictures. It is well known that a surface's topography has a significant impact on a material's bulk characteristics (Assender, *et al*., 2002). After bonding, atoms or molecules work together to produce bulk qualities, which are mechanical characteristics.

The AFM pictures of PVDF-Fe_3O_4 coating surfaces at constant humidity (RH 50%) are displayed in Figure 4,5,6,7. AFM pictures make it clear that the PVDF-Fe_3O_4 surfaces from different collectors have different

morphologies. The surfaces were gathered on the static metal surface and have a rough form (figure 5). As shown in the AFM picture on the 37.5 nm * 37.5 μm lateral area for PVDF-Fe_3O_4 thin film, which is gathered on the revolving drum surface, we noticed that it was made up of microparticles connected by fiber-like connections (figure 5). The alignment structure of a revolving drum is greater than that of a PVDF-Fe_3O_4 sample obtained from a stationary plate. These topological variations may be caused by of stretching polymer molecules by rotation of the polymer species' sputter and collector processes with the surface.

Abbott-Firestone curves are shown in the surfaces' atomic force microscopy (AFM) pictures (see figure 4). The curve that displays the percentage of material provided in relation to the covered area is known as the bearing ratio curve. The vertical axis displays the recorded heights and depths of the surface, while the horizontal axis displays the bearing ratio as a percentage. The percentage of a surface that falls above or below a specific depth is shown by a bearing ratio study. The PVDF-Fe_3O_4 film collected on the revolving drum has a lower Core roughness value (Sk = 164 nm) than the static drum (Sk = 743 nm), as shown by Abbott-Firestone curves. Abbott-Firestone curves, three-dimensional AFM images, and the topography of the PVDF fibers' outer surfaces created at different kinds of collectors demonstrate that an alignment structure

has been seen in the specimens recovered from spinning drums (figure 4, 5). The AFM histograms for the height pictures are displayed in Figure 6. The surface texture is associated with the height distribution histograms. The statistical distribution of the z-values (heights) in a topographical picture is shown by the height histogram. The graph of columns that follow (or bins) is known as a histogram. Each column in the histogram represents a range of heights. The number of picture pixels with a height value within the specified range is shown by the height of each column. The red triangle has been positioned slightly below the surface level, and the blue triangle has been set to the lowest height value in order to calculate the volume of each pit. The height difference between the two peaks, calculated as the average pit depth, is around 0.4 nm. The void volume determined by the histogram for the samples from the static metal plate and revolving drum is 12352 μm^3 and 9194 μm^3, respectively. An imbalance in the height distribution graph was evident in the 3D picture as well as in the rough sample taken from the static drum. In addition to reaching the lowest roughness, the samples from the revolving drum also showed the required uniform height distribution.

The spatial characteristics that determine the surface periodicity and anisotropy include Srwi. The 2D Fourier transform of sample surface maps provides the basis for calculating the spatial parameter. The radial wave

index is known as the Srwi. It displays the size of the main radial wavelength and describes the sample surface's spatial structure. The 2D Fourier map's radial spectrum contained the dominating wavelength (Srw). The amplitude values related to M/(2–1) equally-spaced semi-circles, with the center at the center of the 2D Fourier map, are added up to determine the radial spectrum. The semicircles' radial is expressed in pixels, and r falls between 1 and 2, M/2–1. Compared to a static drum, the dominating wavelength has a higher value for the revolving drum sample. The ratio of the dominant wavelength's average amplitude to total amplitude is known as Srwi. Additionally, Srwi fluctuates between 0 and 1. This value is near zero if the dominating wavelength is present. This value is around 1 in the absence of a dominating wavelength (Tilinova, et al., 2024). Figure 7 shows the radial frequency distributions for PVDF -Fe_3O_4 fibers (10 wt,%) manufactured at two different types of collectors.

By employing several kinds of collectors, various fiber architectures were produced. Figure 8 summarizes the surface characteristics of the AFM image for pristine PVDF-Fe_3O_4 nanofibrous film material utilizing several kinds of drums. Nanofiber mats with random orientation may be produced using a static metal plate, while aligned nanofiber mats could be produced using a spinning drum. Additionally, a metal bar was fastened during the electrospinning process to create a stretching electric field. In this way, the morphology of the PVDF-Fe_3O_4 surfaces was enhanced.

Conclusions

In this study, we produced a pure PVDF-Fe_3O_4 fibrous film substance. From the AFM imaging results, it is evident that the aligned nanofibers were created using the electrospinning approach. To examine their form and structure, we produced highly aligned nanofibrous film material using a directed electric field in electrospinning equipment. We used AFM, or atomic force microscopy. By switching between two different kinds of collectors throughout the electrospinning process, the morphology of the electrospun PVDF-Fe_3O_4 fibers was examined. A static plate may be used to construct nanofiber mats with random orientation, whereas a rotating drum was used to create aligned nanofiber mats. The electrospinning process using a drum that rotates and the presence of an external molecular stretching field will be among the primary topics of the forthcoming studies on nanofibrous PVDF-Fe_3O_4 coated composite material.

Figure 1. 10 wt,% PVDF-Fe_3O_4 nanofibrous material preparation steps: a) PVDF solution preparation with hot plate, ultrasonic bath and plastic syringe, b) electrospinning equipment

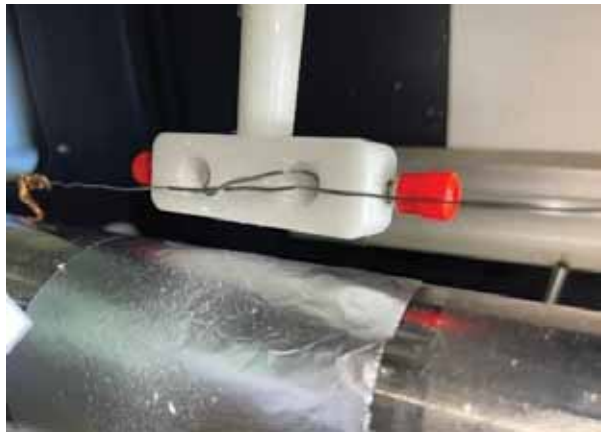

Figure 2. Joining metal bar to the electrospinning equipment

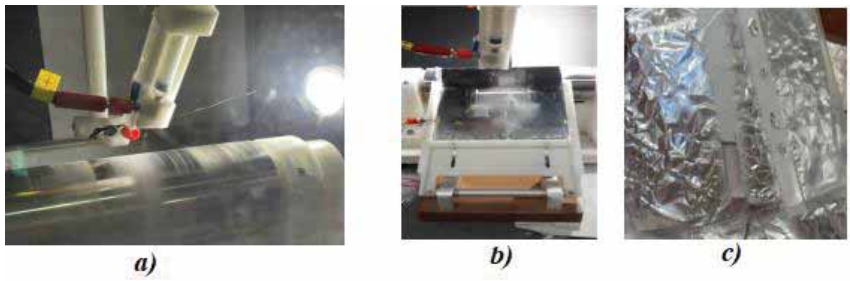

Figure 3. Using different types of collectors in electrospinning (Voltage - 16 kV): a) Rotating drum (Rotating Drum speed = 556 rpm; b) Static metal plate c) 10 wt, % PVDF-Fe_3O_4 nanofibrous sample on the surface of aluminum foil.

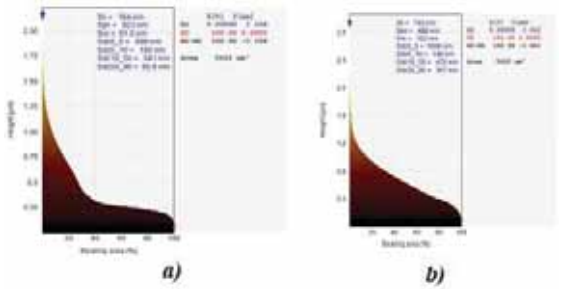

Figure 4. The Abbott-Firestone curve for PVDF-Fe_3O_4 (10 wt, %) fibers prepared at different types of collectors: (a) sample from rotating drum, (b) sample from static drum**.**

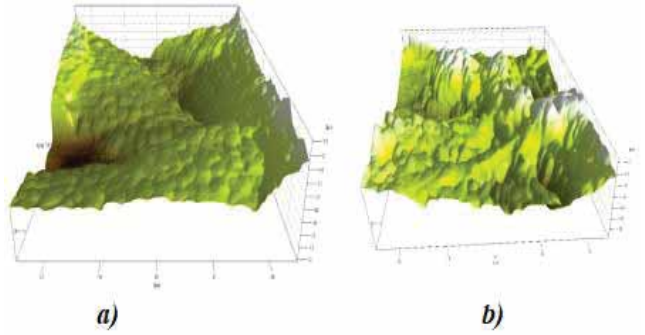

Figure 5. Three-dimensional AFM images of the outer surfaces of the PVDF-Fe_3O_4 fibers (10 wt, %) prepared at different type of collectors: (a) sample from rotating drum, (b) sample from static drum.

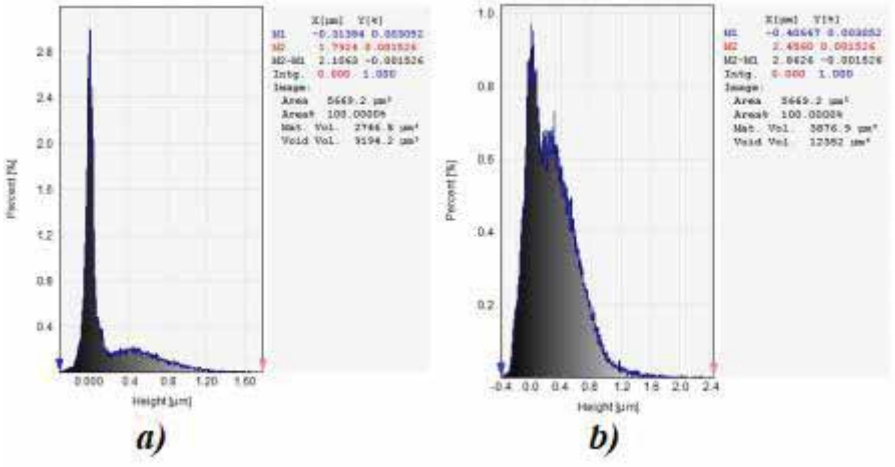

Figure 6. Surface roughness study histograms of the height distribution graphs of PVDF-Fe_3O_4 fibers (10 wt,%) made at various collector types: (a) a revolving drum sample; (b) a static drum sample. The image's minimal

height is shown by the blue cursor, while the bearing plane or surface level is indicated by the red cursor marker, which is positioned directly below the higher peak.

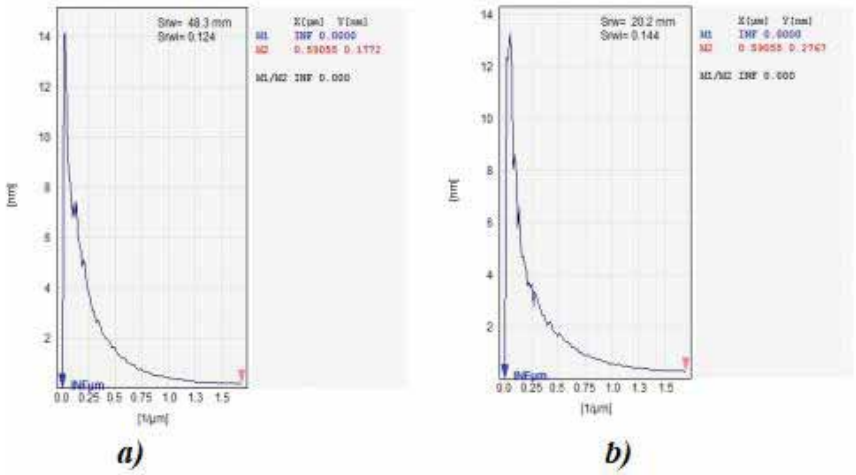

Figure 7. Radial Frequency profile for PVDF-Fe_3O_4 fibers (10 wt, %) prepared at different types of collectors: (a) sample from rotating drum, (b) sample from static drum

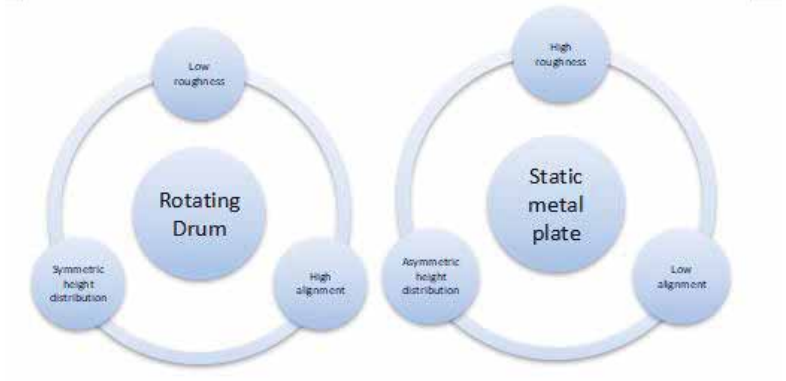

Figure 8. Summarization for AFM image surface parameters of PVDF-Fe_3O_4 fibers (10 wt, %) prepared at different types of collectors.

References

Jayakumar, O.D., Mandal, B.P., Majeed, J., Lawes, G., Naik, R., & Tyagi, J. M. (2013). Inorganic–organic multiferroic hybrid films of Fe3O4 and PVDF with significant magneto-dielectric coupling. 1, 3710–3715.

Prabhakaran, T., & Hemalatha, J. (2013). Ferroelectric and magnetic studies on unpoled poly (vinylidine fluoride)/Fe3O4 magnetoelectric nanocomposite structures. Mater. Chem. Phys. 37:781–787.

Huang, Z.Q., Zheng, F., Zhang, Z., Xu, H.T. & Zhou, K.M. (2012) Performance of the PVDF-Fe3O4 Ultrafiltration Membrane and the Effect of a Parallel Magnetic Field Used during the Membrane Formation. Desalination, 292, 64-72.

Chen, D., Li, J., Yuan, Y., Gao, C., Cui, Y., Li, S., Liu, X., Wang, H., Peng, C., Wu, Z. A. (2021). Review of the Polymer for Cryogenic Application: Methods, Mechanisms and Perspectives. Polymers 2021, 13, 320.

Bhattacharjee, S., Mondal, S., Banerjee, A., & Kumar, K. (2020). Chattopadhyay. Souvik Bhattacharjee, Suvankar Mondal, Anibrata Banerjee, and Kalyan Kumar Chattopadhyay, Mater. Res. Express 7. Mater. Res. Express 7, 044001.

Samadi, A., Hosseini, S.M., & Mohseni, M. (2018). Investigation of the electromagnetic microwaves absorption and piezoelectric properties of electrospun Fe3O4-GO/PVDF hybrid nanocomposites. Org. Electron. 59, 149–155.

Martins, P., Lopes, A.C. & Lanceros-Mendez, S. (2014). Electroactive Phases of Poly (Vinylidene Fluoride): Determination, Processing and Applications. Progress in Polymer Science, 39, 683-706.

Tasaka, S., & Miyata, S. (1985). Effects of crystal structure on piezoelectric and ferroelectric properties of copoly (vinylidenefluoride-tetrafluoroethylene). J Appl Phys 57:906–910.

Ting, Y., Gunawan, H., Sugondo, A., & Chiu., C.W. (2013). A New Approach of Polyvinylidene Fluoride (PVDF) Poling Method for Higher Electric Response. Ferroelectrics, 446, 28–38.

Chowdhury, T., D'Souza, N., & Dahotre, N. (2021). Low-Cost Reliable Corrosion Sensors Using ZnO-PVDF Nanocomposite Textiles. Sensors, 21, 4147.

Chowdhury, T., D'Souza, N., Ho, Y.H., Dahotre, N., & Mahbub, I. (2020). Embedded Corrosion Sensing with ZnO-PVDF Sensor Textiles. Sensors, 20, 3053.

Mansouri, S., Sheikholeslami, T.F., & Behzadmehr, A. (2019). Investigation on the electrospun PVDF/NP-ZnO nanofibers for application in environmental energy harvesting. J Mater Res Technol, 8: 1608–1615.

Ghosal, K., Chandra, A., Praveen, G., Snigdha, S., Roy, S., Agatemor, C., Thomas, S., & Provaznik, I. (2018). Electrospinning over Solvent Casting: Tuning of Mechanical Properties of Membranes. Sci. Rep. 2018, 8, 5058. Sci. Rep. 2018, 8, 5058.

Meng, Z., Zhu, L., Wang, X., & Zhu, M. (2023). Electrospun Nanofibrous Composite Membranes for Separations February, Accounts of Materials Research 4(2).

Xue, J., Wu, T., Dai, Y., & Xia, Y. (2019). Electrospinning and Electrospun Nanofibers: Methods, Materials, and Applications, Chem Rev. 24; 119(8): 5298–5415.

Terada, D., Kobayashi, H., Zhang, K., Tiwari, A., Yoshikawa, Ch., & Hanagata, N. (2012). Transient ChargeMasking Effect of Applied Voltage on Electrospinning of Pure Chitosan Nanofibers from Aqueous Solutions. Sci. Technol. Adv. Mater, 13, 015003.

Tong, H-W., & Wang, M. (2012). Negative Voltage Electrospinning and Positive Voltage Electrospinning of Tissue Engineering Scaffolds: A Comparative Study and Charge Retention on Scaffolds. Nano LIFE, 2, 1250004.

Hu, J., Wang, X., Ding, B., Lin, J., Yu, J., & Sun, G. (2011). One-Step Electro-Spinning/Netting Technique for Controllably Preparing Polyurethane Nano-Fiber/Net. Macromol. Rapid Commun, 32, 1729–1734.

Demir, M.M., Yilgor, I., Yilgor, E., & Erman, B. (2002). Electrospinning of Polyurethane Fibers. Polymer, 43, 3303–3309.

Ayres, C., Bowlin, G., & Henderson S. (2006). Modulation of anisotropy in electrospun tissue-engineering scaffolds: analysis of fiber alignment by the fast fourier transform, Biomaterials, 27 (32): 5524–5534.

Nitti, P., Gallo, N., Natta, L., Scalera, F., Palazzo, B., Sannino, A., & Gervaso, F. (2018). Influence of Nanofiber Orientation on Morphological and Mechanical Properties of Electrospun Chitosan Mats, Hindawi Journal of Healthcare Engineering, Article ID 3651480, 12 pages.

Mishra, S., Mohanty, Z., & Nayak, S.K. (2023). Study of nonisothermal crystallization kinetics of unstretched and uni-axially stretched electroactive PVDF composite films, Macromol. Chem. Phys. 224 - 2200326.

Sun, L.L., Li, B., Zhang, Z.G., & Zhong, W.H. (2010). Achieving very high fraction of β-crystal PVDF and PVDF/CNF composites and their effect on AC conductivity and microstructure through a stretching process, Eur. Polym. J. 46: 2112–2119.

Kim, J. F., Jung, J. T., Wang, H. H., Lee, S. Y., Moore, T., Sanguineti, A., Drioli, E., & Lee, Y.M. (2016). Microporous PVDF membranes via thermally induced phase separation (TIPS) and stretching methods. Journal of Membrane Science, 509, 94-104.

Martins, P., Lopes, A.C., & Lanceros-Mendez, S. (2014). Electroactive phases of poly (vinylidene fluoride): Determination, processing and applications. Polym. Sci. 39, 683.

Harstad, S., D'Souza, N., Soin, N., El-Gendy, A.A., Gupta, S., Pecharsky, V.K., Shah, T., Siores, E., & Hadimani, R.L. (2017). Enhancement of $\boldsymbol{\beta}$-phase in PVDF films embedded with ferromagnetic Gd5Si4 nanoparticles for piezoelectric energy harvesting AIP Adv. 7, 056411.

Ruan, L., Yao, X., Chang, Y., Zhou, L., Qin, G., & Zhang, X. (2018). Properties and Applications of the ? Phase Poly (vinylidene fluoride). Polymers 10, 1.

Ahn, Y.C., Park, S.K., Kim, G.T., Hwang, Y.J., Lee, C.G., Shin, H.S., & Lee, J.K. (2006). Development of high efficiency nanofilters made of nanofibers. Curr. Appl. Phys. 6, 1030 (2006)

Lannutti, J., Reneker, D., Ma, T., Tomasko, D., & Farson, D. (2007). Electrospinning for tissue engineering scaffolds. Mater. Sci. Eng. C 27, 504.

Hunley, M.T., & Long, T.E. (2008). Electrospinning functional nanoscale fibers: a perspective for the future. Polym. Int. 57, 385.

Zhou, Z., & Wu, X.F. (2015). Electrospinning superhydrophobic–superoleophilic fibrous PVDF membranes for high-efficiency water–oil separation Mater. Lett. 160, 423–42794

Assender, H., Bliznyuk, V., & Porfyrakis, K. (2002). How Surface Topography Relates to Materials' Properties, Science, 297(5583): 973-976.

Tilinova, O.M., Inozemtsev, V., Sherstyukova, E., Kandrashina, S., Pisarev, M., Grechko, A., Vorobjeva, N., Sergunova, V., & Dokukin, M.E. (2024). Cell Surface Parameters for Accessing Neutrophil Activation Level with Atomic Force Microscopy. Cells, 13, 306.